Armed Services Technical Information Agency

Because of our limited supply, you are requested to return this copy WHEN IT HAS SERVED YOUR PURPOSE so that it may be made available to other requesters. Your cooperation will be appreciated.
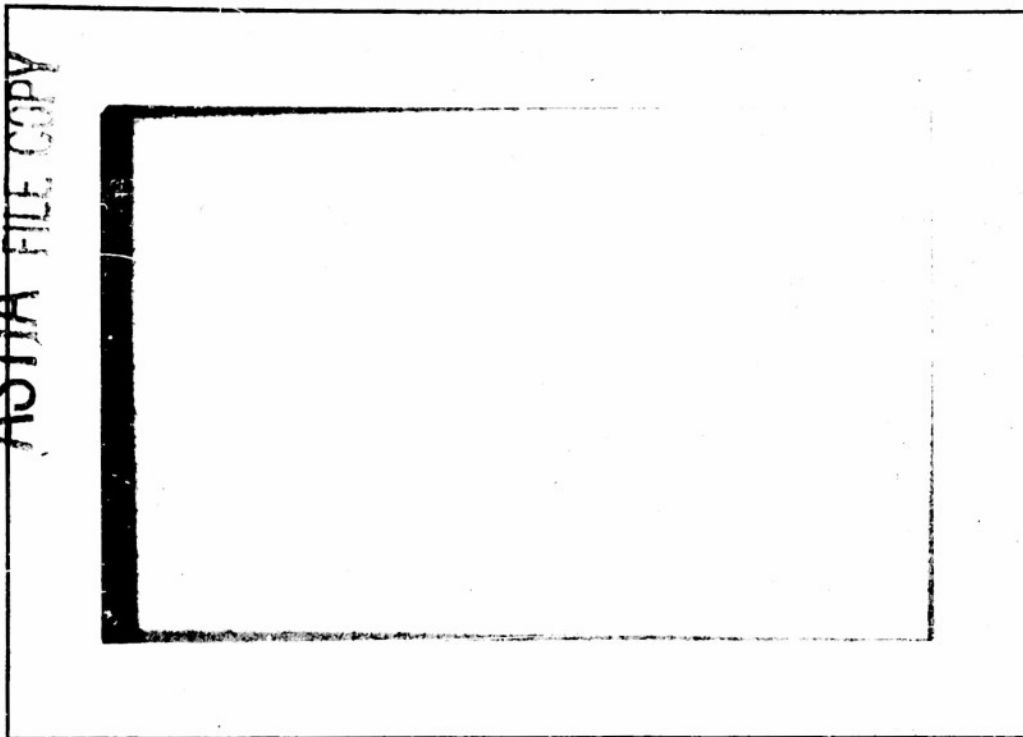
AD
43707

UNCLASSIFIED

COSMIC RAY GROUP

Department of Physics

UNIVERSITY OF MINNESOTA

CERENKOV COUNTER MEASUREMENT

OF COSMIC RAY ALPHA PARTICLES AT 41°

by

Nahmin Horwitz

TECHNICAL REPORT

August, 1954

Department of Physics
University of Minnesota
Minneapolis, Minnesota

CERENKOV COUNTER MEASUREMENT

OF COSMIC RAY ALPHA PARTICLES AT 41°

a thesis submitted to the Graduate Faculty of the University

of Minnesota

by

Nahmin Horwitz

in partial fulfillment of the requirements for the degree of

Doctor of Philosophy

University of Minnesota
Minneapolis, Minnesota
1954

SUMMARY

Knowledge of the flux and energy spectrum for each charge component of primary cosmic rays will be helpful in solving the fundamental problem of their origin. In the latitude-sensitive region of energies, the spectra can be determined by a series of flux measurements at different latitudes.

A Cerenkov counter was flown by balloon to a height of 16 gm/cm^2 on February 2, 1954, at a geomagnetic latitude of 41° 21'. The purpose of the experiment was to measure the alpha particle flux and to observe the behavior of a Cerenkov counter in the $3 \leq Z \leq 9$ region. A Cerenkov counter was used because of its inherent discrimination against slow particles. Guard counters were included to identify background events due to side showers. Crossed trays of Geiger counters were used to identify background events in which a proton interacted in the radiator, producing a number of charged secondaries.

The equipment was at altitude for 355.5 minutes. The pulse height distribution for all events showed a partially resolved alpha peak. A total of 3024 events occurred which gave pulse heights corresponding to alpha particles. In 451 of these cases a guard counter was fired simultaneously. These are all classed as background. In 898 of the cases two or more Geiger counters in one of the crossed trays were fired simultaneously. Out of the 898 there is evidence that 247 represent true alphas which either 1) interacted in matter beneath the radiator, 2) produced a delta ray which triggered a second Geiger counter, or 3) passed obliquely through two adjacent Geiger counters. The remaining 651 are classed as background due to proton-induced nuclear interactions. It is estimated that an additional 478 events were due to background that the other two devices did not detect.

SUMMARY   continued

There remains after substracting the background 1444 events believed to be due to primary alphas. These lead to the value 99 particles/m^2 - steradian - second for the flux of alpha particles at the top of the atmosphere at 41°. The estimated uncertainty in this figure is $\pm$ 16%.

In the CNO region there is an indication of partially resolved carbon and oxygen peaks but this is not certain. There is evidence that the geometry factor of the telescope was appreciably increased due to the action of delta rays. The data is consistent with saying that most events which give Cerenkov pulses corresponding to $Z \neq 6$ are, in fact, associated with a heavy particle, but in the Li, Be, B region there is a background due to proton-induced interactions.

INDEX

INDEX (continued)

LIST OF ILLUSTRATIONS

LIST OF ILLUSTRATIONS (continued)

PART I   PURPOSE OF THE EXPERIMENT

The experiment which is the subject of this thesis had as its primary goal the determination of the flux of alpha particles in cosmic rays at a geomagnetic latitude of $41°$. As a secondary goal, it was hoped that something would be learned regarding the usefulness of a Cerenkov counter for flux measurements on the cosmic ray components with charge $3 \leq Z \leq 9$.

PART II   MOTIVATION FOR THE EXPERIMENT

1) The multiply charged components and reasons for their study

At the present time it is generally accepted that cosmic rays are simply very high energy atomic nuclei. We became aware of the components with charge greater than one in 1948 when Freier[1] et. al. sent photographic emulsions and cloud chambers to the top of the atmosphere by balloon and observed heavy tracks due to fast multiply charged particles.

Since that time various experimenters have attempted to get more detailed information about the heavy components. Ultimately one would like to know the flux and energy spectrum of each charge component, as this kind of information should be very helpful in solving the fundamental problem of the origin of cosmic rays.

For example, if we find that Li, Be, and B are absent in the primary cosmic rays we may conclude that the heavier components $(Z \geq 6)$ must have come from a source which is no more than a small fraction of a collision mean free path from the earth.

We would like to know in general the relative abundances of all nuclei
in cosmic rays in order to compare them to the relative abundances
found elsewhere in the universe.

Knowledge of the energy spectra and their variation with charge
may tell us something about the accelerating mechanism. If the energy
spectrum of each heavy component is the same but the spectrum for
protons is different, one might suspect an acceleration mechanism which
is sensitive to the charge to mass ratio since that quantity is
approximately 1/2 for all heavies, but 1 for protons.

Similarly the energy spectra may tell us something of the history
of the cosmic ray during its travels to us from its source. In Fermi's
theory[2] the shape of the spectrum is intimately connected with the
average lifetime of the cosmic ray. According to his first theory,
magnetic fields kept cosmic rays in the galaxy until they died by
collisions with hydrogen in interstellar space. Since different charge
components have appreciably different collision mean free paths, it
would follow that average lifetimes and thus shapes of energy spectra
would vary continuously and rather appreciably among the different
charge components. In his later theory[3], the galaxy was assumed to be
so leaky that the life of a cosmic ray was usually ended by its leaving
the galaxy rather than by collision. The galaxy was equally leaky for
all heavy components. Thus this theory implied that they would have
lifetimes, and therefore energy spectra, which were independent of charge.

In addition, it will be very interesting to see if all charge
components show a knee similar to that in the total flux spectrum.

We would also like information on time variations, for when one
deals with heavies one knows he is dealing directly with primaries.
Therefore, time variations if they exist would be particularly
significant.

One would also want to know if time variations differed for different components.

2) Reasons for doing a counter experiment

The integral energy spectrum for a heavy component in the range $0 \leq E_t \leq 7.6$ Bev/nuc. can be determined by a series of flux measurements at different geomagnetic latitudes. This follows from the fact that there is a known cut-off energy associated with each geomagnetic latitude. Thus the value of the flux at a given latitude is also the value of the integral energy spectrum corresponding to the particular cut-off energy involved. A knowledge of the integral energy spectrum also leads to a value of the total flux. Thus the problem reduces to a series of flux measurements.

These measurements can be made by photographic emulsions, cloud chambers, or various kinds of counters. A typical counter does not give as much detailed information about a single event as does the photographic emulsion, and, as will be discussed under the section dealing with past experimental difficulties, it is subject to types of background which don't bother an emulsion. On the other hand, a counter experiment has the following advantages:

1) high counting rates are more feasibly obtained

2) the time of occurrence of each event is easily recorded

3) the analysis of the data is relatively fast and easy

The experiment described in this thesis was a counter experiment.

3) Reasons for concentrating on the alpha component

While ideally we would like detailed information for every charge component, some are easier to study than others. Thus, in an emulsion experiment there is reason for concentrating on the highly charged components—namely because they leave a large track and are, therefore, relatively easy to find and identify. For counter experiments on the

other hand, the Z equals 2 or alpha particle component seems to be the easiest to study. For one thing, alpha particles are the most abundant heavy component. There are 10 times more alphas than all other heavy components combined. This is of great practical importance because in cosmic ray work one is so often plagued by the problem of insufficient counting rate. This is especially true if one wants to look for time variations. There is also the problem of resolution. In a counter experiment one uses some quantity like energy loss to identify the charge of the particle passing through the equipment. One then makes a frequency distribution plot of the results and hopes to see resolved peaks corresponding to each charge component. If, as has usually been the case, the percentage resolution is roughly constant for all peaks and the property being measured goes as the square of the charge, then the peaks will get crowded closer and closer together as one goes out to larger charge components. Thus, in this respect there is the best hope of seeing a resolved alpha peak, since the alphas have the lowest charge of all the heavies.

Alphas have a charge to mass ratio of 1/2, which is the same as that of the other heavy components, and have a mean free path in interstellar hydrogen which is appreciably shorter than that for protons. Thus they are rather typical heavies and their study should lead to information characteristic of all heavies.

PART III   PAST MEASUREMENTS OF THE ALPHA FLUX

1) Summary of methods and results

In past attempts to measure the alpha flux, emulsions, cloud chambers, inefficient Geiger counters, scintillation counters, and proportional counters have been used. With so many independent methods

of attack we could have had great confidence in the results if they had agreed, but unfortunately most of the experiments lacked precision. Table 1 summarizes some of the results.

TABLE I   Summary of some past measurements of the alpha flux

geomag. latitude	cut-off energy (total in Bev/nuc.)	method	experimenter	flux (particles per m^2 per sec. per ster.)
0	7.6	inefficient Geiger counter	Singer[4]	14+20
30	4.9	emulsion	Goldfarb[5] et. al.	60+10
41	2.75	proportional counter	Perlow[6] et. al.	110+20
41	2.75	inefficient Geiger counter	Singer[7]	140+60
	1.67	cloud chamber	Linsley[8]	135+20
51	1.54	emulsion	Goldfarb[5] et. al.	340+120
55	1.30	scintillation counter	Ney et. al.[9]	340
55	1.30	proportional counter	Davis et.al.[10]	310+30
55	1.30	cloud chamber	McDonald[11]	230+60

Over the latitude-sensitive region, the integral energy spectrum for the total flux is approximated quite closely by:

(equation 1) $I(E_t) = \dfrac{K}{(E_t)^{1.0}}$

where:

E_t is the total energy of the particle

$I(E_t)$ is the flux of particles with energy greater than E_t

Since most cosmic rays are protons, it is generally assumed that the protons have an inverse power law energy spectrum with exponent equal to 1 also. This assumption is correct unless, as was pointed out by Kaplon et. al.[12], the total flux measurements included a large amount of albedo (the higher energy protons would make relatively more albedo and this would tend to flatten the total flux spectrum). In any case, the value 1.0 is a lower limit for the exponent in the proton energy spectrum.

Similar attempts to fit the CNO and $Z \geq 10$ components indicate a value of 1.4 for the exponent in their energy spectra [12]. The alphas would probably be expected to have an integral energy spectrum with exponent between the limits 1.0 and 1.4. Figure 1 is a graph of the results listed in table 1. The dotted lines are not attempts at best fits to the data but rather show the slopes corresponding to the values 1.0 and 1.4. As can be seen, the precision of the data is not even good enough to decide between what we expect are the two limiting values.

2) Problems involved in getting a precise value for the alpha flux

In order to get a precise value for the alpha flux one must be able to clearly identify the alphas. In most of the past experiments one measured the rate of energy loss of the cosmic ray as it passed through the detector. At sufficiently low latitudes all primaries are relativistic, and this energy loss will simply be proportional to the
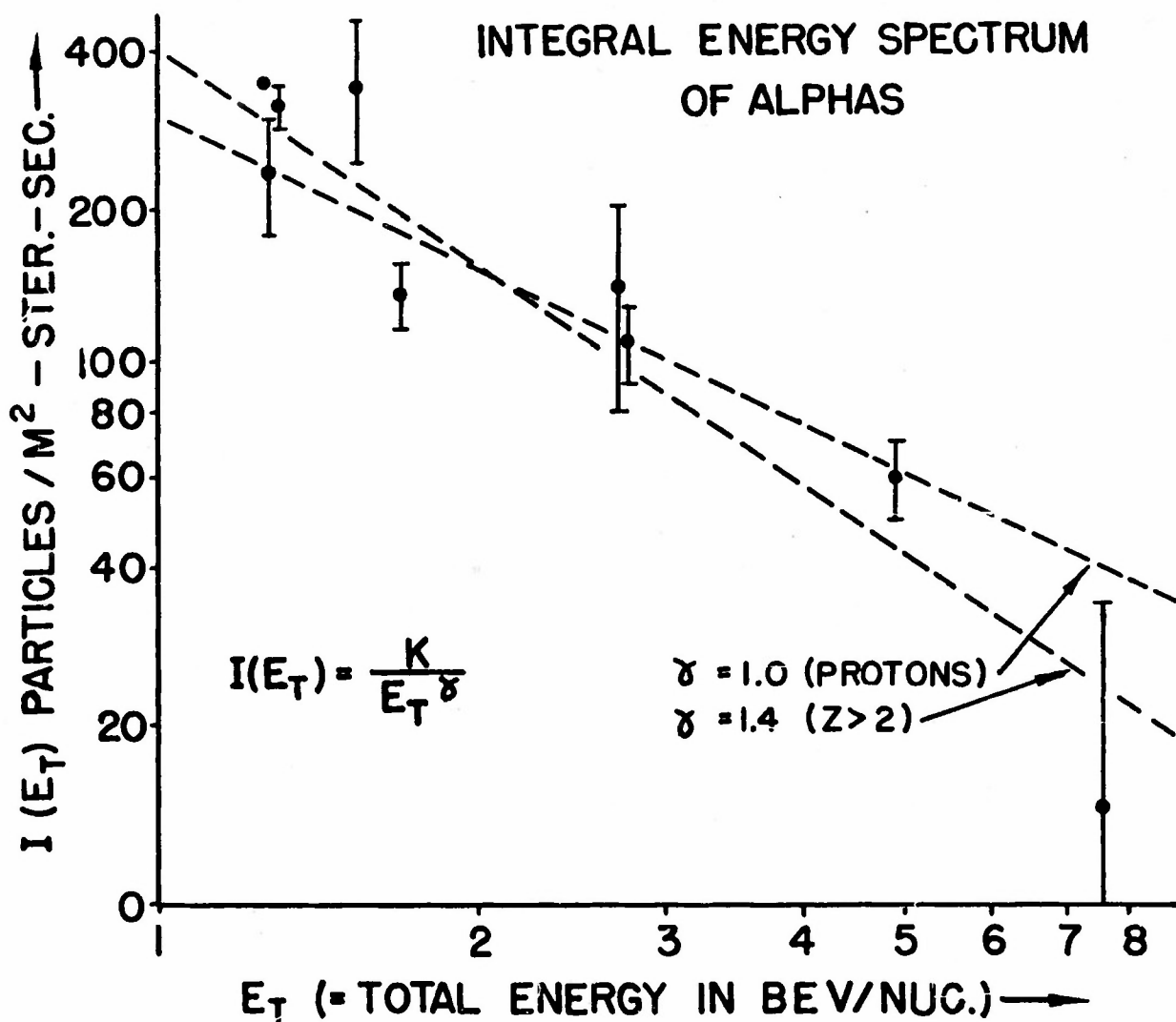
FIGURE 1   The points represent flux values measured at various geomagnetic latitudes. The values of E_t are the cut-off energies at the corresponding latitudes. The dotted lines have slopes corresponding to $\gamma = 1.0$ and 1.4 in the spectrum $I(E_t) = K/E_t^{\gamma}$

square of the charge. One then makes a frequency distribution plot
and expects to see a clearly resolved peak in the region of energy losses
corresponding to alphas. Unfortunately this never happens. There is
always a background to confuse the issue. In fact in many cases this
background has been so big that no peak whatever was observed. Now what
causes the background? For one thing, regardless of latitude, unless
the equipment is above the atmosphere, it will be looking at a beam of
slow secondary particles of charge one in addition to primary particles.
Even if the detector is above the atmosphere, it may be looking at some
slow albedo. Some of these slow particles will be ionizing near four
times minimum and will therefore look like primary alphas. In principle
experimenters using emulsions can eliminate this problem by restricting
their analysis to long tracks and following every track far enough to
establish that the particle is not slowing down. This involves a
considerable amount of work and as far as I know has not been done in
a comprehensive way.

Counter experiments not only had the above mentioned problem but
the following in addition. They had background due to nuclear interactions
within the counter. That is, a proton came in, interacted, and the
combined energy loss of the products of the interaction was of the same
order as the energy loss from a single alpha. It is true that the
probability of such an interaction is small, but the flux of protons is
so much larger than the flux of alphas that the number of these interactions
can be a significant fraction of the number of alphas which are being
measured. Counter experiments also had background due to showers of
singly charged particles which originated in the air above the detector.
Finally, the alpha peak could be smeared out because of fluctuations in
the energy lost by similar particles or fluctuations in the response of
the detector to events in which the particles lose the same amount of

energy. Fluctuations become serious if they cause the tail of the proton curve to extend into the alpha region.

There is some evidence that the most serious contributor to background is slow secondaries. A number of experiments which did not attempt to discriminate against slow particles also did not obtain any alpha peak. On the other hand, the Naval Research Laboratory group which flew proportional counters[6,10] included absorbers in their telescopes to eliminate slow particles, and did succeed in partially resolving the alpha peak. In addition the experiment which will be described in this thesis and a recent experiment by Bohl[13] had provision to eliminate slow particles, and both succeeded in partially resolving the alpha peak.

PART IV   THE CERENKOV COUNTER AND ITS APPLICATION TO FLUX MEASUREMENTS

There is an alternative to including an absorber in the equipment, because there is a counter which, in effect, has the absorber built in. This device is a Cerenkov counter. When a charged particle passes through a medium with velocity greater than the velocity light has in the medium, a small amount of light is radiated.

Let:

N be the number of quanta emitted

ω be the angular frequency

x be the path length in the medium

n be the refractive index of the medium

β be the velocity of the particle in units of c

Z be the charge of the particle in units of the electronic charge

α be the fine structure constant $\left(= e^2/\hbar c^2 \right)$

then[14]:

(equation 2)
$$\frac{d}{d\omega}\left(\frac{dN}{dx}\right) = Z^2 \frac{\alpha}{c}\left[1 - \frac{1}{n^2\beta^2}\right]$$

As with energy loss the amount of Cerenkov radiation depends on the velocity and charge of the particle. As with energy loss the amount of radiation varies as the square of the charge. It is the velocity dependence that is different. In fact, it is almost opposite. The amount of Cerenkov radiation is zero if the velocity of the particle is below the cut-off value, which is the velocity of light in the medium, and rises rapidly to a saturation value as the velocity increases and β approaches one. This is a very important point. If alphas are identified by measuring ionization loss, slow particles interfere because they have a larger ionization loss than fast ones. (And in fact they may have the same energy loss as an alpha.) But if one uses Cerenkov radiation, slow particles don't interfere at all because they give less radiation than fast ones. Figure 2 shows the variation of Cerenkov light with velocity of the incident particle for lucite.

The Cerenkov counter seems like an inviting tool for counter measurements in the CNO region also. Here background usually was due to nuclear interactions in which a few evaporation particles lost a great deal of energy and gave very large pulses. In a Cerenkov counter this kind of interaction would be harmless. In order to give as much light as an oxygen nucleus the interaction would have to produce essentially 64 fast mesons. For this reason, while the experiment to be described was designed principally to measure the alpha flux, provision was made to get some idea of the behavior of the counter in the $3 \le Z \le 9$ region.

Cerenkov counters had been used for balloon flight experiments during the past few years by Winckler and Anderson[15] in their studies of the albedo problem. They developed a counter which used a slab of lucite 20 cm thick as the radiator and a side-window photomultiplier as the detector.

CERENKOV RADIATION IN LUCITE (n = 1.50)

$L = N(\beta)/N(1)$

$\beta = v/c$

$\gamma = $ TOTAL ENERGY/REST ENERGY
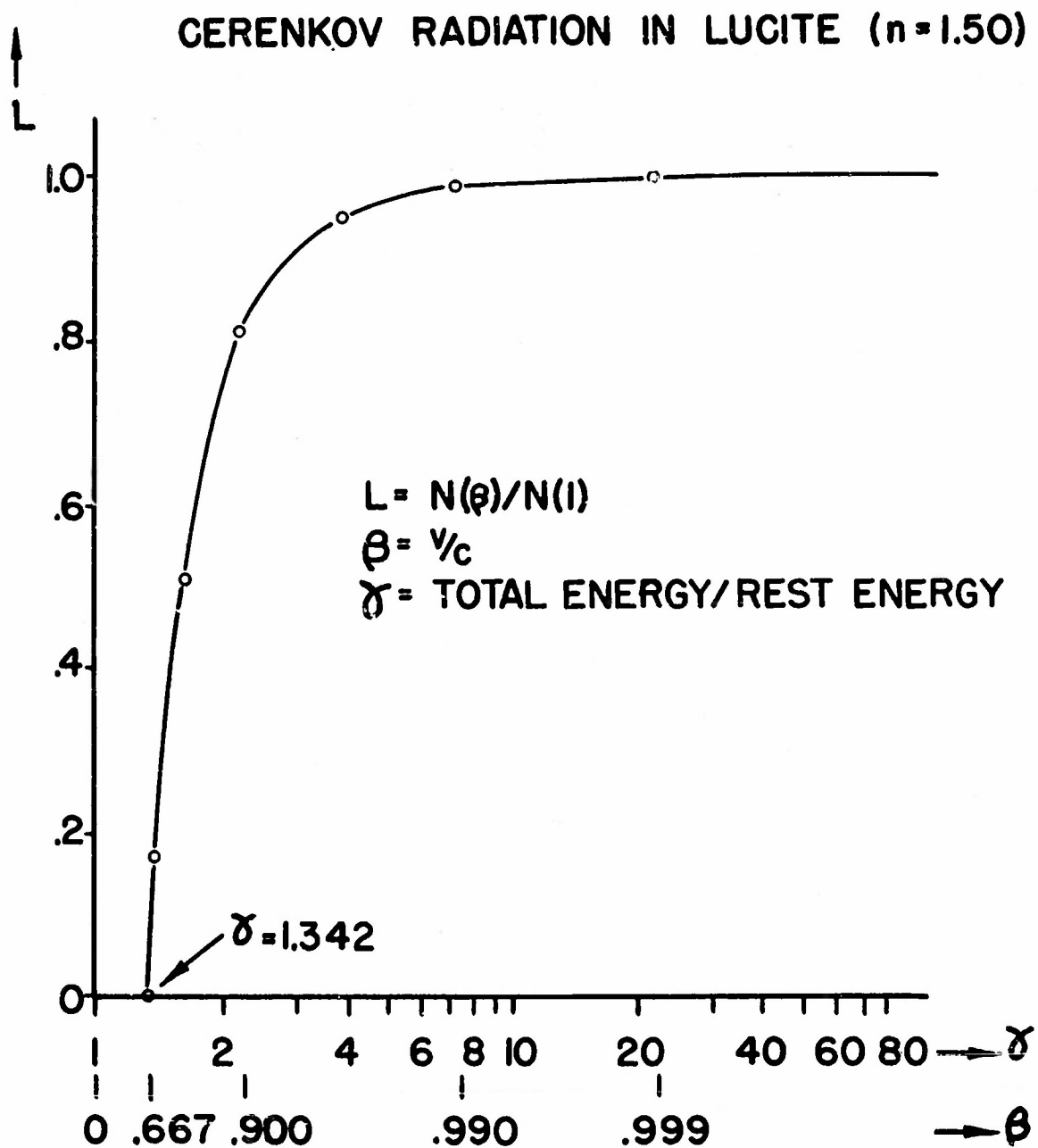
$\gamma = 1.342$

FIGURE 2.   L is the amount of Cerenkov light emitted by a particle with velocity β or energy γ, relative to that emitted by a particle with $\beta = 1$. No light is emitted unless $\beta \geq 1/n$ ($\gamma \geq 1.342$ for lucite).

Linsley[8] then adapted the Cerenkov counter to measurements of multiply charged primaries by experimenting with thinner lucite radiators. In a flux measurement of the lighter multiply charged components, it is desirable that the radiator be as thin as possible in order to reduce background due to nuclear interactions. On the other hand, thin radiators reduce the amount of light obtained. The saturation value for a fast proton in lucite is approximately 300 photons of visible light per cm of path length. This is a factor of about 100 less light than one obtains from an equal thickness of a good scintillator. Only a small percentage of these photons are converted into photoelectrons. This presents a real problem. The number of photoelectrons appears to be Poisson distributed and if the mean were too small the fluctuations would smear adjacent charge peaks together. This of course, would be disastrous. Linsley found that a reasonable compromise was obtained with a radiator 2 1/2 cm thick. He used a rather small Cerenkov counter to trigger a cloud chamber. I then built a somewhat larger Cerenkov counter which also utilized a lucite radiator 2 1/2 cm thick and used it in a purely counter measurement of the alpha flux. The rest of this thesis will deal with a description of the equipment and the results. The experiment is the outgrowth of work begun by Ney. Several years ago he developed the first scintillation counter equipment suitable for balloon flight flux measurements of heavies[9]. This is the same type of experiment but uses a Cerenkov counter instead of a scintillation counter.

PART V   DESCRIPTION OF THE EQUIPMENT

In essence the equipment consists of a Geiger counter telescope to define a solid angle in space from which particles will be accepted, a

Cerenkov counter to determine their charge, some devices to identify background events, and apparatus to record the information obtained.

1) The Geiger counter telescope

Trays A, B, and C which are shown in solid black in Figure 3 form the Geiger counter telescope. The equipment records only those events which cause a coincidence between these three trays. Tray A consists of two Victoreen thin wall (30 mg/cm^2) aluminum counters. Thin wall counters were deemed advisable in order to reduce nuclear interactions occurring just above the radiator. These counters were .745" in diameter and had a quoted active length of 2 3/4". Tray B and Tray C each contained eight counters. They were made of copper; had wall thickness of .022", outside diameter of 1", and nominal length of 8".

If f_v is the flux of particles coming from the vertical and N is the observed counting rate, then:

$$\text{(equation 3)} \quad N = Gf_v$$

where G is a constant determined by the geometry of the telescope. The geometry factor for this telescope was determined in two ways, by direct calculation and by using the observed counting rate in a presumably known flux. The details of these calculations are given in appendix A. The value obtained for the geometry factor is 9.5 ± 1 cm^2-steradian.

2) The Cerenkov counter

Between trays A and B (figure 3) is the Cerenkov counter. The radiator is a cylindrical slab of lucite 4" in diameter and 1"thick. The lucite is optically coupled by a film of mineral oil to the cathode of a Dumont K1198 photomultiplier. The K1198 is an end-window photomultiplier with a 5" diameter photocathode. This tube was operated with the cathode at ground potential and the collecting anode at plus 1220 volts. A positive output signal was taken from the 10th dynode,

4 GUARD COUNTERS

LUCITE RADIATOR 1" THICK

5" DUMONT PHOTOMULTIPLIER

TRAY A 1.5"x 2.75"

TRAY B TRAY C 8"x 8"

CERENKOV COUNTER TELESCOPE
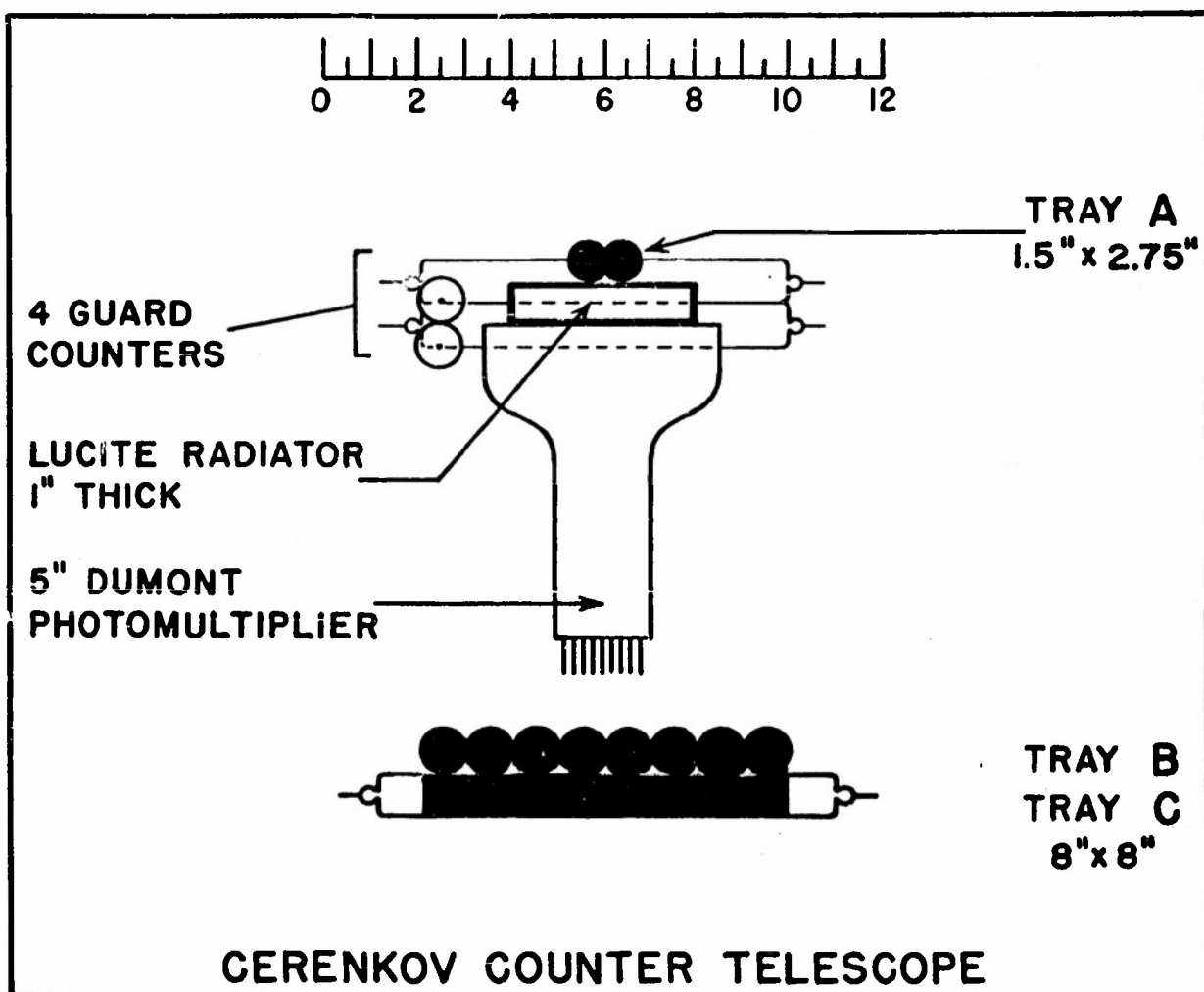
FIGURE 3

amplified, and displayed on a cathode ray tube. It is assumed that the
deflection on the CRT is proportional to the voltage output of the
photomultiplier which in turn is proportional to the amount of Cerenkov
light made in the lucite. This means of course that the amplifiers
must be linear, and it also means that the pulses from the photomultipler
must be free of saturation effects. The Dumont tubes are presumably
free of saturation for signals in which the instantaneous currents are
less than 12 ma.[16] Let i be tube current and approximate the current
pulse by a square wave, then:

$$\text{(equation 4)} \qquad i = CV_o / t$$

where:

C = output capacity of the tube

V_o = output voltage signal

t = duration of the pulse in the photomultiplier (the time it takes

   for C to charge up to a voltage V_o)

The Cerenkov light is emitted essentially instantaneously, but spread
in transit time gives t a finite value. Assuming $t \geq 5 \cdot 10^{-9}$ seconds
and C equal $10 \mu\mu f$, equation 4 shows that the instantaneous current
will be less than 12 ma if the output signals are less than 6 volts.
The amplifiers were designed so that the maximum signal required
(i.e. full scope deflection) was 5 volts.

Since during a flight the equipment takes different orientations
in the earth's magnetic field, it is important that the gain of the
photomultiplier should not be affected by a magnetic field. A Dumont
K1197 (same as the K1198 except the photocathode has a 3" diameter)
was tested, and a field stronger than the earth's field did not affect
its gain. The test is described in Appendix B. The Dumont K 1198
which was actually used was not tested, but both tubes have the same
dynode structure.

3) Crossed Geiger counter trays and guard counters

As has been stated the Cerenkov counter discriminates against slow protons. In the same way it discriminates against nuclear interactions in which a few slow evaporation particles are given off. However, it does not discriminate against an interaction in which high energy mesons are made. Thus if a proton comes in, interacts in the top of the lucite, and four fast mesons come off, the detector not knowing any better will indicate that an alpha came through. The same thing would happen if a narrow shower of fast particles originating in the air above the apparatus passed through the detector. In order to identify these events as background, an attempt was made to make the detector indicate whenever more than one particle passed through the telescope. This was done by placing the Geiger counters in tray B perpendicular to those in tray C and having an electronic circuit which would indicate whenever more than one Geiger counter was tripped simultaneously in either tray. Since there were 8 Geiger counters in each tray, the bottom 64 square inches was effectively divided into 64 separate units, and the detector could tell whenever particles passed through more than one of these units simultaneously.

In a further attempt to determine which events were really due to alphas and which to background, four guard counters were placed alongside the lucite radiator to detect side showers.

4) The method of recording

Figure 4 illustrats the method of recording. The pulses from the photomultiplier are amplified and then fed to the vertical deflection plates of a cathode ray tube. The CRT, however, is normally cut off. A coincidence between trays A, B, and C produces an enabling gate which is applied to the grid of the CRT and turns it on. A camera takes continuous pictures of the CRT. Thus, if a single fast particle passes

TRAY A

TRAY B

TRAY C

COINCIDENCE
CIRCUIT

CIRCUIT TO
DETECT WHEN
>I COUNTER
IS FIRED

PHOTOMULTIPLIER

AMPLIFIER

GUARD
COUNTERS
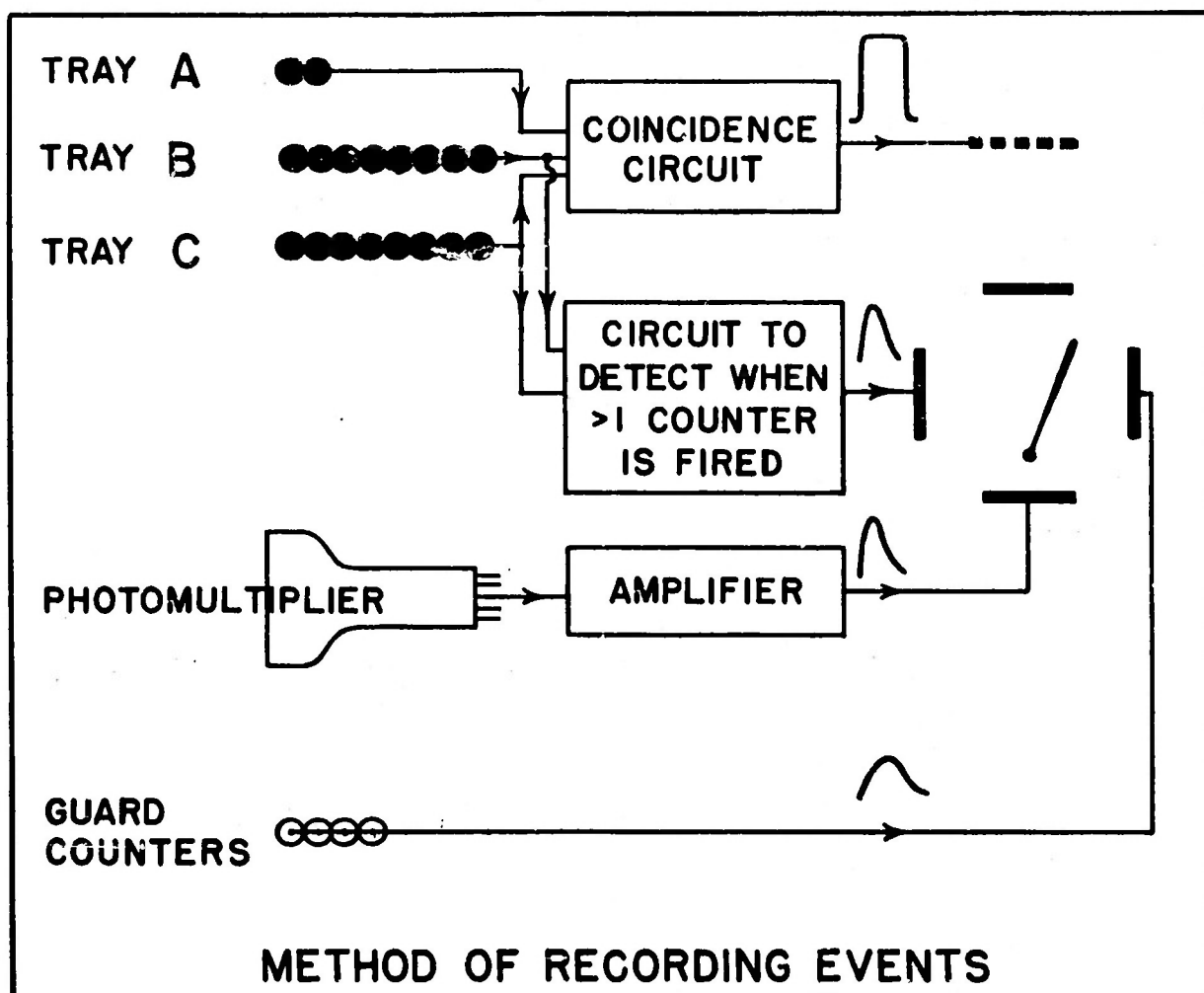
METHOD OF RECORDING EVENTS

FIGURE 4

through the telescope a vertical line, whose height is proportional to the square of the charge of the particle, will be recorded on the film.

The outputs of both tray B and tray C are also fed to a circuit which detects those cases in which more than one Geiger counter in a tray is fired simultaneously. When this happens a signal is fed to one of the horizontal deflection plates. When a guard counter is triggered a signal is fed to the other horizontal deflection plate. Thus, if a nuclear interaction takes place the pulse on the film will appear tipped to one side, and if a side shower takes place it will be tipped to the other side. Figure 4 shows a pulse on the CRT tipped to the right. A pulse like this on the film would imply the following: First, something must have triggered trays A, B, and C simultaneously or the CRT would not have been turned on. Second, some fast particle passed through the lucite radiator and emitted an amount of Cerenkov radiation proportional to the vertical height of the pulse. Finally, the fact that the pulse is tipped to the right shows that a particle also passed through one of the guard counters.

5) Electronics

Let h be pulse height. Let h_o be the mean pulse height corresponding to a fast proton. It was desired to record pulses where h/h_o ranged from 0 to 80. In order to do this, 2 cathode ray tubes were used (like 2 scales on a voltmeter). One tube covered the range $0 \le h/h_o \le 9$ and the other covered the range $0 \le h/h_o \le 80$.

Figure 5 shows a block diagram of the amplifier system. The output of the photomultiplier is fed to a shaping circuit which slows down the leading edge and lengthens the pulse. This is done 1) to make sure the pulse does not reach its maximum until after the enabling gate has turned on the cathode ray tubes, and 2) because a slower pulse on the CRT is easier to photograph.
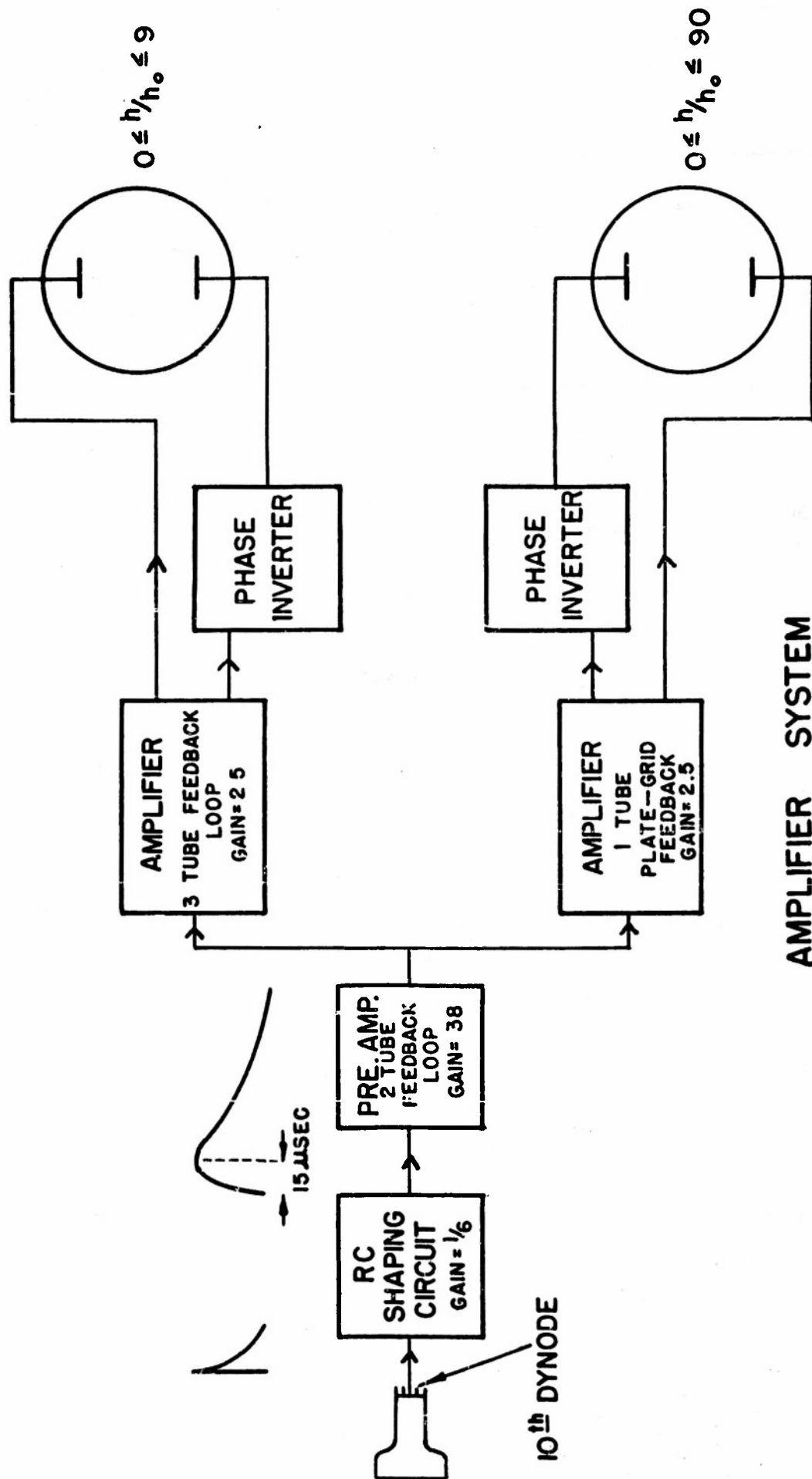
AMPLIFIER SYSTEM

FIGURE 5.

The amplifiers had considerable inverse feedback to improve linearity and stability. (A balloon experiment requires minimum battery weight and B+ voltage is apt to decrease by 10 to 20% during a flight.) Single tubes with plate to grid feedback, and 2 and 3 tube feedback loops as described in Elmore and Sands[17] were used. The calibration of the system is discussed in Appendix C.

The essentials of the coincidence circuit are shown in figure 6. Diodes were used for power economy. It is believed that the circuit had a resolving time of approximately 4 microseconds. The 3-fold to 2-fold ratio was 7:1. The output of the coincidence circuit triggered a flip-flop which produced a positive gate which turned on both cathode ray tubes.

The circuit which detected when 2 or more geiger counters in either trays B or C were triggered simultaneously is also shown in figure 6. A Geiger counter tray is itself an adding circuit. It has a fixed capacity into which is fed an amount of charge proportional to the number of Geiger counters which are discharged. Thus the signal voltage out of tray B or tray C is proportional to the number of Geiger counters which have been discharged. What is needed then is a circuit which will subtract from each signal an amount equivalent to the signal produced when one Geiger counter is fired. Then if any signal remains it means that more than one Geiger counter was fired. This subtraction is accomplished by using a diode, biased off an amount equal to the signal obtained when one Geiger counter is discharged.

6) Power requirements: pressure, time and temperature data: flight gondola

The total power requirements for the electronic circuits was about 25 watts. The filaments were supplied by one Willard ER 40-6, six volt storage cell. It had a rated capacity 25% higher than what was needed for one 8 hour flight. Eveready #482 dry cells were used to supply B+ voltage. Voltage for the Geiger counters, cathode ray tubes,

COINCIDENCE

CIRCUIT

CIRCUIT TO DETECT WHENEVER MORE THAN ONE GEIGER COUNTER IN TRAYS B OR C ARE TRIGGERED SIMULTANEOUSLY

100 μ SEC

30V

CLIPPER

FLIP FLOP

AMP.

CATHODE RAY TUBE GRID

15 μ SEC.

AMP.

STRETCH

HORIZONTAL DEFLECTION PLATE

$(n-1)$ V

nV

22 K

IN38

560 K

+6V

IN 38

100 K

−30

−V

47 K

SIMILAR CIRCUIT

TRAY A

B

C
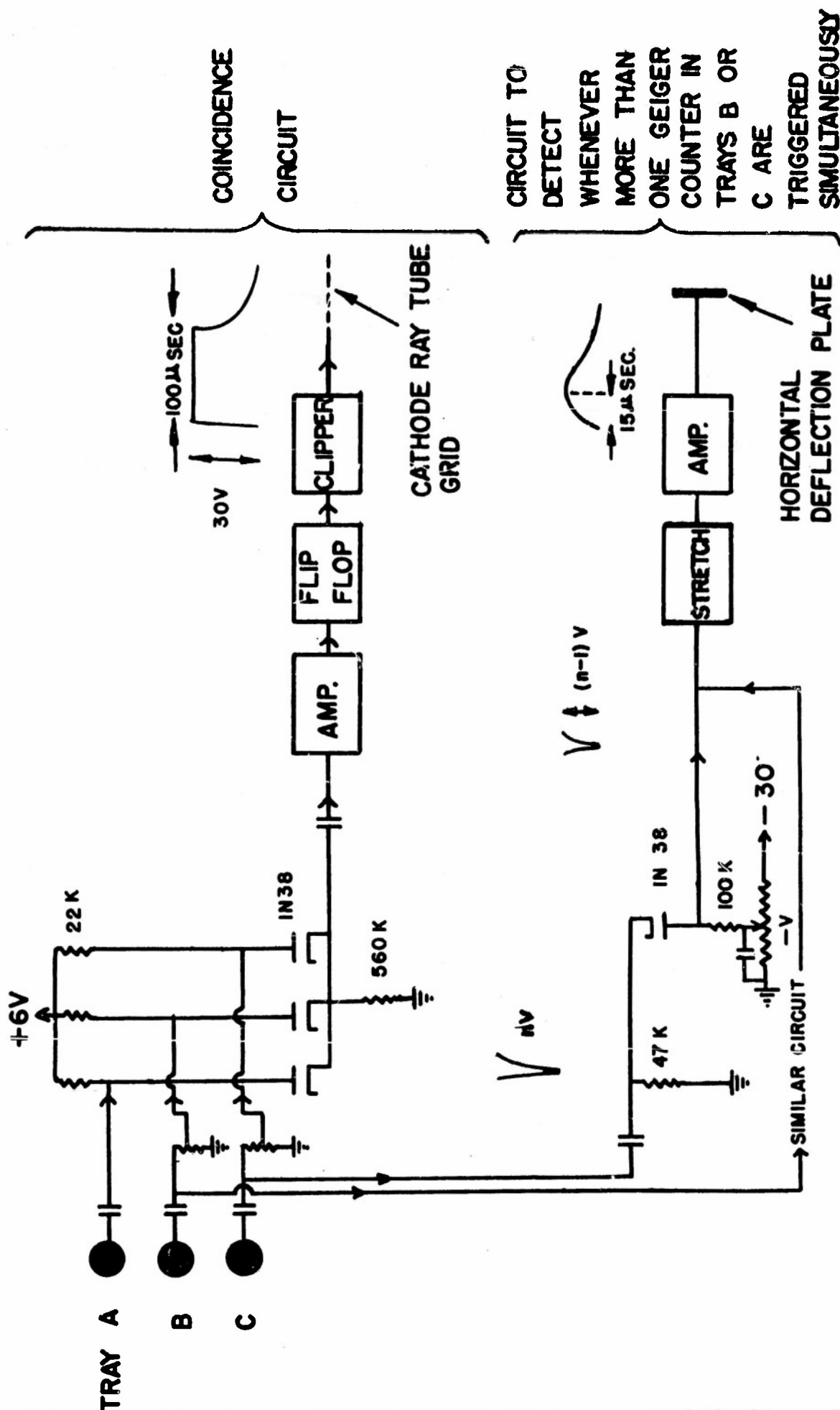
FIGURE 6.

and photomultiplier was obtained from stacks of Eveready #413 miniature 30v dry cells.

A watch with a second hand, a thermometer, and a Wallace and Tiernan pressure guage were mounted on an instrument panel which was photographed by the same camera which photographed the cathode ray tubes. The camera lens was always open and a light would flash on the instrument panel (but not on the cathode ray tubes) once every minute.

All the equipment was mounted in a spherical gondola whose diameter was $30''$ and whose wall thickness was $.03''$. The gondola was pressure tight and thus the equipment remained in one atmosphere of pressure during the flight. (This was to prevent corona discharge.) The Wallace and Tiernan guage was connected by a hose to a lead-through fitting in the wall of the gondola.

Figures 7, 8, and 9 are photographs of various parts of the equipment.

23
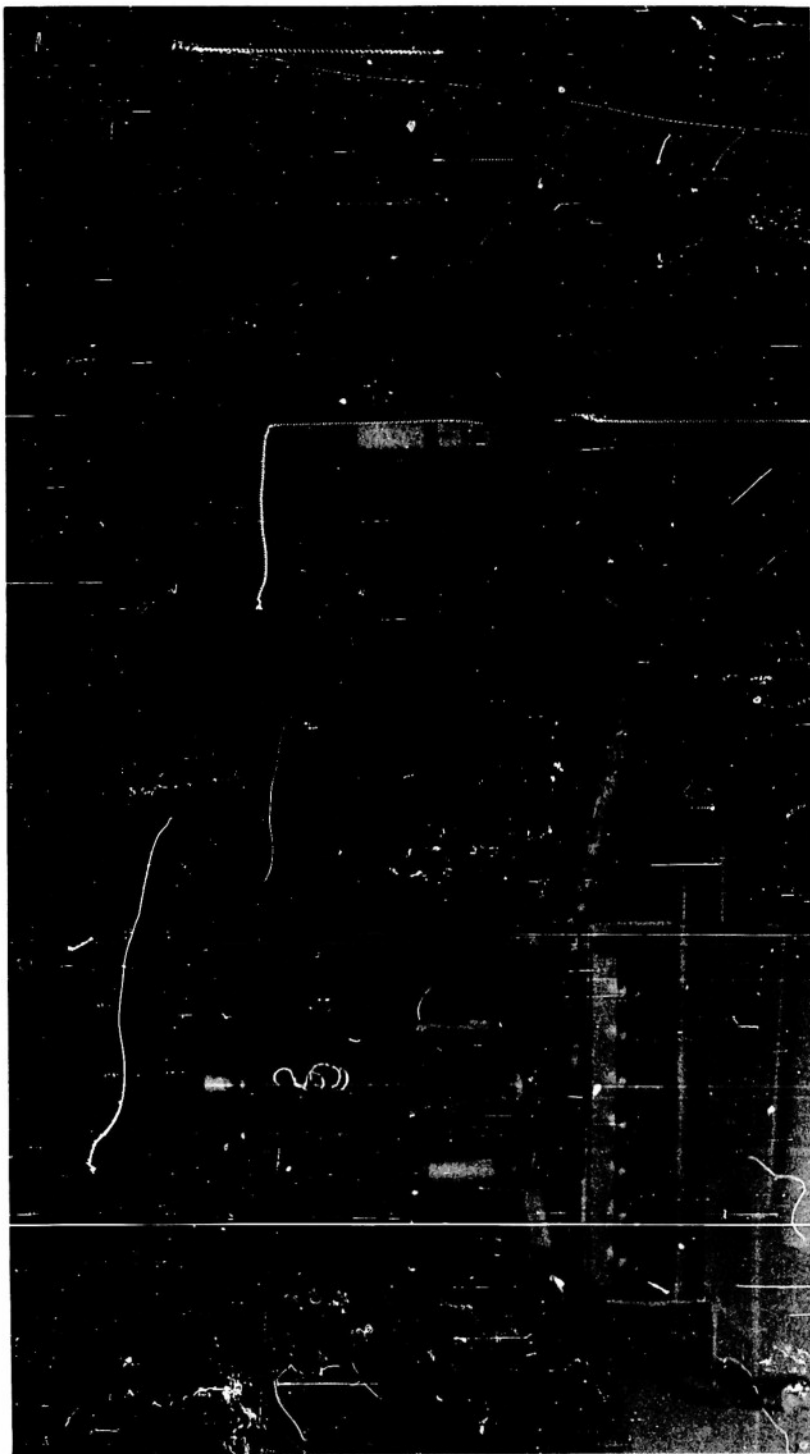
FIGURE 7.   Elements of the Cerenkov counter and the Geiger counter telescope.
To the left are the Dumont photomultiplier which is plugged into the pre-amplifier
chassis, Geiger counter trays B and C, and two guard counters. To the right is
the lucite radiator, Geiger counter tray A, and two more guard counters.
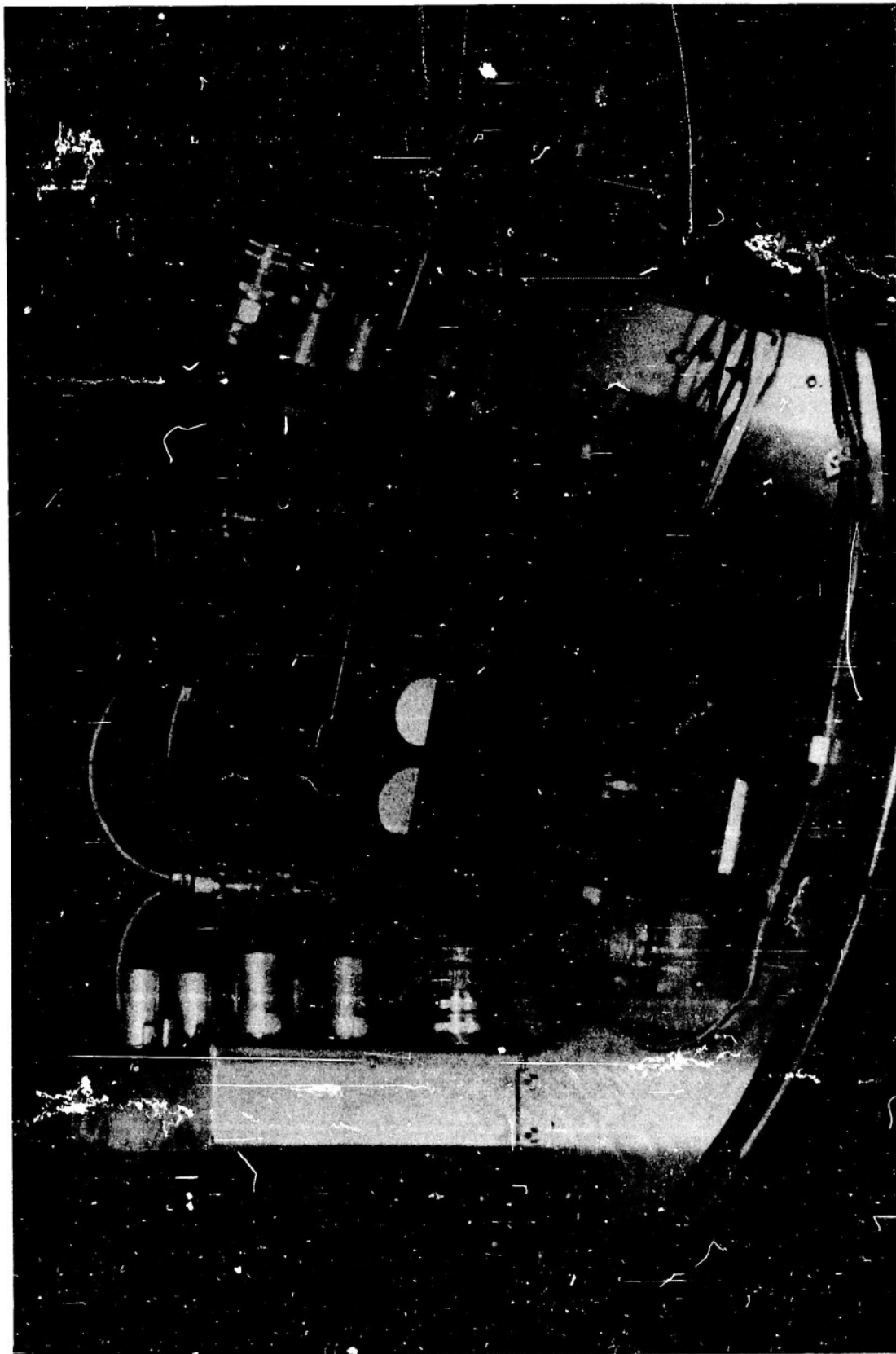
FIGURE 8.   The recording apparatus.   The two chassis contain amplifier and coincidence circuits.   In the center are the two cathode ray tubes, and the instrument panel.   The object in the foreground (with the wing nut) is the camera.
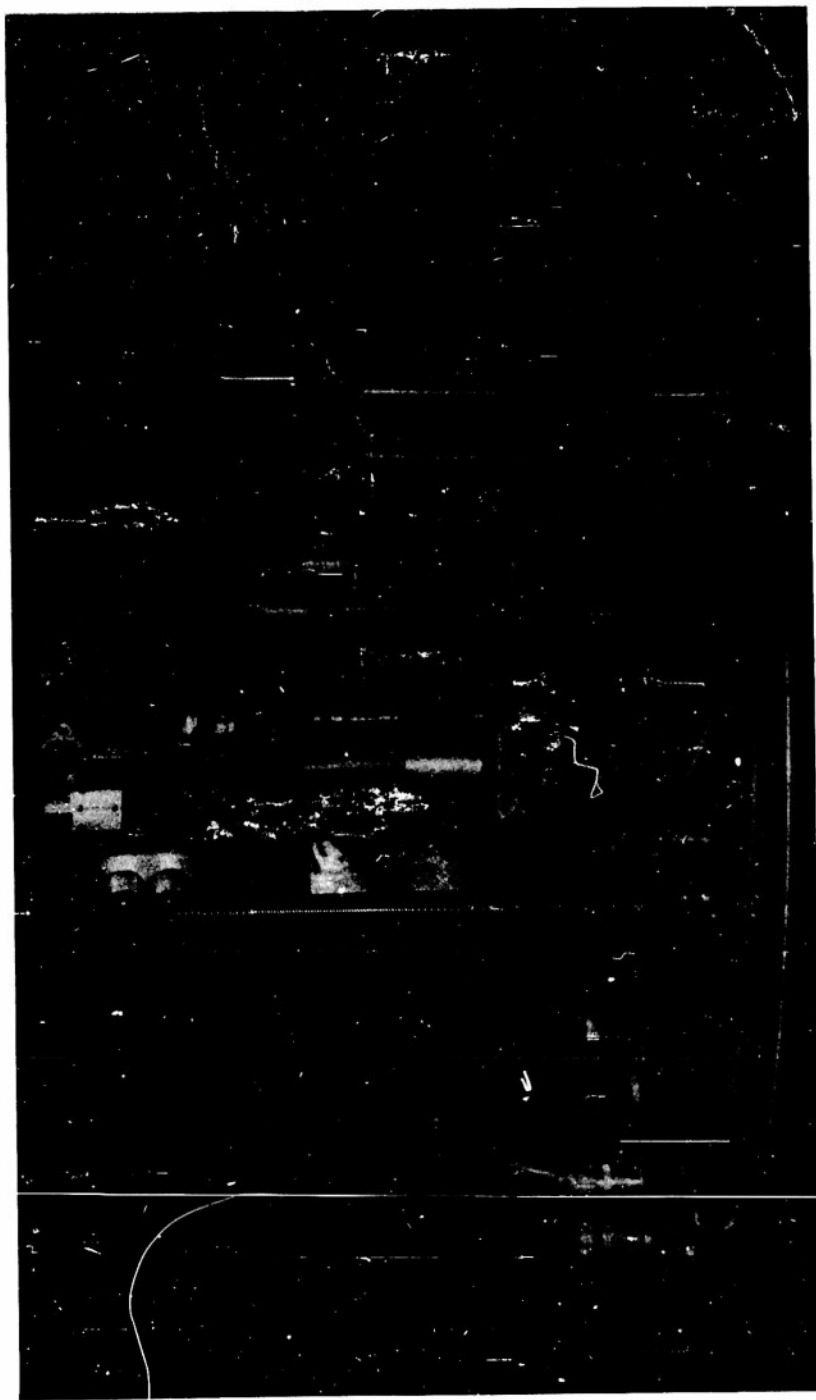
FIGURE 9.   The Cerenkov counter, Geiger counter telescope, and recording apparatus fully assembled.   The circular plate on which the equipment is mounted was placed inside a spherical aluminum gondola which in turn was attached to the balloon.

PART VI   RESULTS

1) Pulse height distribution for sea level mesons and the predicted
    shape of the alpha peak

When the apparatus is operated at sea level it is responding to
fast μ mesons. The pulse height distribution obtained is shown in
figure 10. The dotted curve represents a Poisson distribution of mean
30. The fit appears to be quite good. That this is a reasonable result
can be seen as follows: The spectral response of the photomultiplier
has its half maximum values at 3500A and 5700A. In this frequency
range we find from formula 2 that 700 photons are emitted in the 1 inch
slab of lucite by a very fast meson. Assuming a collection efficiency
of 75% we find that we would have on the average 30 photoelectrons
emitted from the photocathode if the conversion efficiency is 6%. This
is the right order of magnitude for the conversion efficiency.

Whereas the average number of photoelectrons may be 30, the actual
number emitted in any one event fluctuates. The conversion process is
of the "yes-no" type; this is very often encountered in physics and
leads naturally to a Poisson distribution as can be seen from the
following argument: First approximate the group of n incoming photons
having various frequencies by a group of n photons all having some
average effective frequency. When a photon enters the photocathode it
either ejects a photoelectron or it doesn't. Let p be the probability
that a photon does eject a photoelectron. Each photon is independent,
i.e. the probability of photon "b" making a photoelectron is quite
independent of whether or not photon "a" succeeded. Now the probability
of getting exactly k photoelectrons is just the probability that exactly
k out of the n photons will have "successes". This probability is
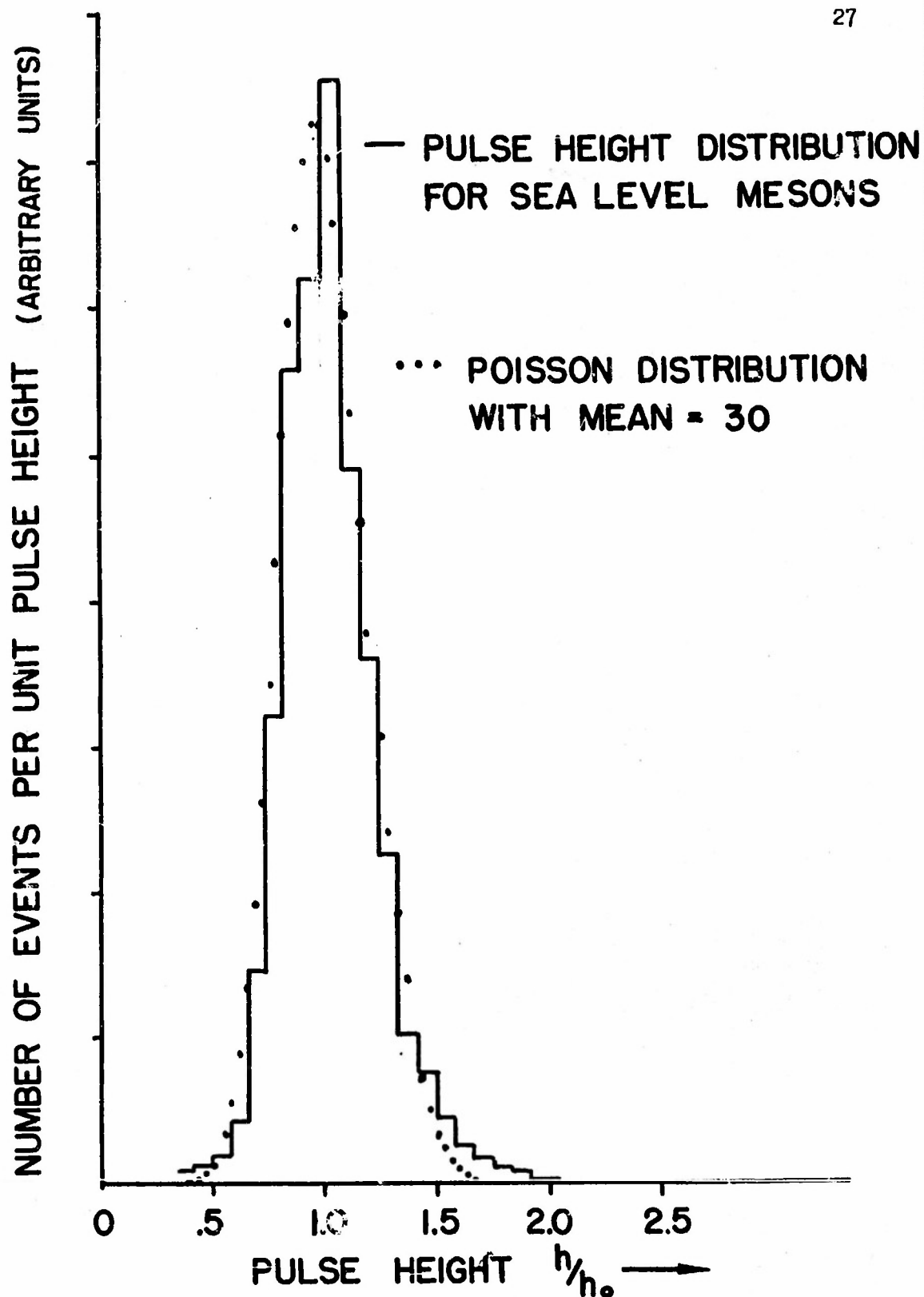
$$p^k \, (1-p)^{n-k} \, c_n^k$$

FIGURE 10. The pulse height distribution for sea level mesons can be fitted quite closely by a Poisson distribution with mean 30. (The disagreement at the peak is probably due to the effects of personal bias in measuring the pulse heights.)

where C_n^k is the number of combinations of n things taken k at a time. This is the binomial probability distribution. It can be closely approximated by a Poisson distribution with mean np if $p \ll 1$ and $n \gg 1$[18]. The reason for making this approximation is that the Poisson distribution is somewhat easier to handle analytically. Thus when one deals with a situation in which the result is the sum of a large group of similar but independent "yes-no" events and if the probability of a "yes" is small compared to unity, one should expect the result to be Poisson distributed.

There are other fluctuations which affect the pulse height distribution, but they are assumed to be negligible compared to the effect of photon statistics.

As will be seen later it is useful to have a crude idea of the region of pulse heights in which alphas are expected to lie. Knowing the shape of the meson or Z equals 1 peak, it is possible to estimate the shape of the alpha or Z equals 2 peak.

Since a fast Z equals 1 particle leads on the average to 30 photoelectrons, a fast Z equals 2 particle would lead to 120 photoelectrons, and if there were no other significant sources of fluctuations the alpha peak should follow a Poisson distribution with mean 120. There is another source of fluctuations, however, due to the fact that at Texas not all alphas are fast. The cut-off kinetic energy at 41° geomagnetic latitude is 1.75 Bev/nuc., and from equation 2 (or figure 2) we find that a particle with this energy gives 87% of the saturation amount of Cerenkov light. Thus at Texas the alpha particles will give amounts of Cerenkov light varying between 87 and 100% of the saturation value. These variations must be folded in with the fluctuations in the number of photoelectrons if one wants to predict the shape of the alpha peak. This is done crudely in appendix D. The

result, which will be used later on, is that essentially no alphas
will give pulses less than 2.7 h_0 and only a few percent will give pulses
greater than 5.4 h_0.

2) The balloon flight

The equipment was flown by balloon from San Angelo, Texas on February
2, 1954. It reached an altitude of 16 gm/cm^2 at 9:30 c.s.t. and remained
there until 3:28 c.s.t.. (The altitude was constant to within 1 gm/cm^2.)
At 3:28 the equipment, suspended from a parachute, was released from the
balloon and floated to earth. When the balloon reached altitude its
geographic location was latitude 31° 9', longitude 100° 30'. At the
end of the flight it had drifted primarily eastward to latitude 31° 59',
longitude 91° 2'. The equipment was recovered in good condition near
Jackson, Mississippi and was returned to San Angelo on February 14. At
that time its operating characteristics appeared to be the same as before
the flight.

3) Results at altitude in the region $0 \leq h/h_0 \leq 9$

Figure 11 shows the pulse height distribution of all events with
pulse heights in the range $0 \leq h/h_0 \leq 9$. This distribution includes all
events in which a guard counter was discharged and all events in which
more than one particle passed through the telescope.

It seems fairly clear that there is a group of pulses due to fast
Z equals 1 particles, a group due to fast Z equals 2 particles, and a
group representing background. The Z equals 1 peak is very large
compared to the Z equals 2 peak, which simply points up the difficulty
in measuring the alpha flux if there is any tendency for proton events
to produce pulses in the alpha region.

Figure 12 shows an enlarged view of the pulse height distribution
in the alpha region. The shaded lines are drawn at h equals 2.7 h_0
and 5.4 h_0. As was mentioned above, all but a small percentage of the
alphas are expected to lie within these limits. The area under
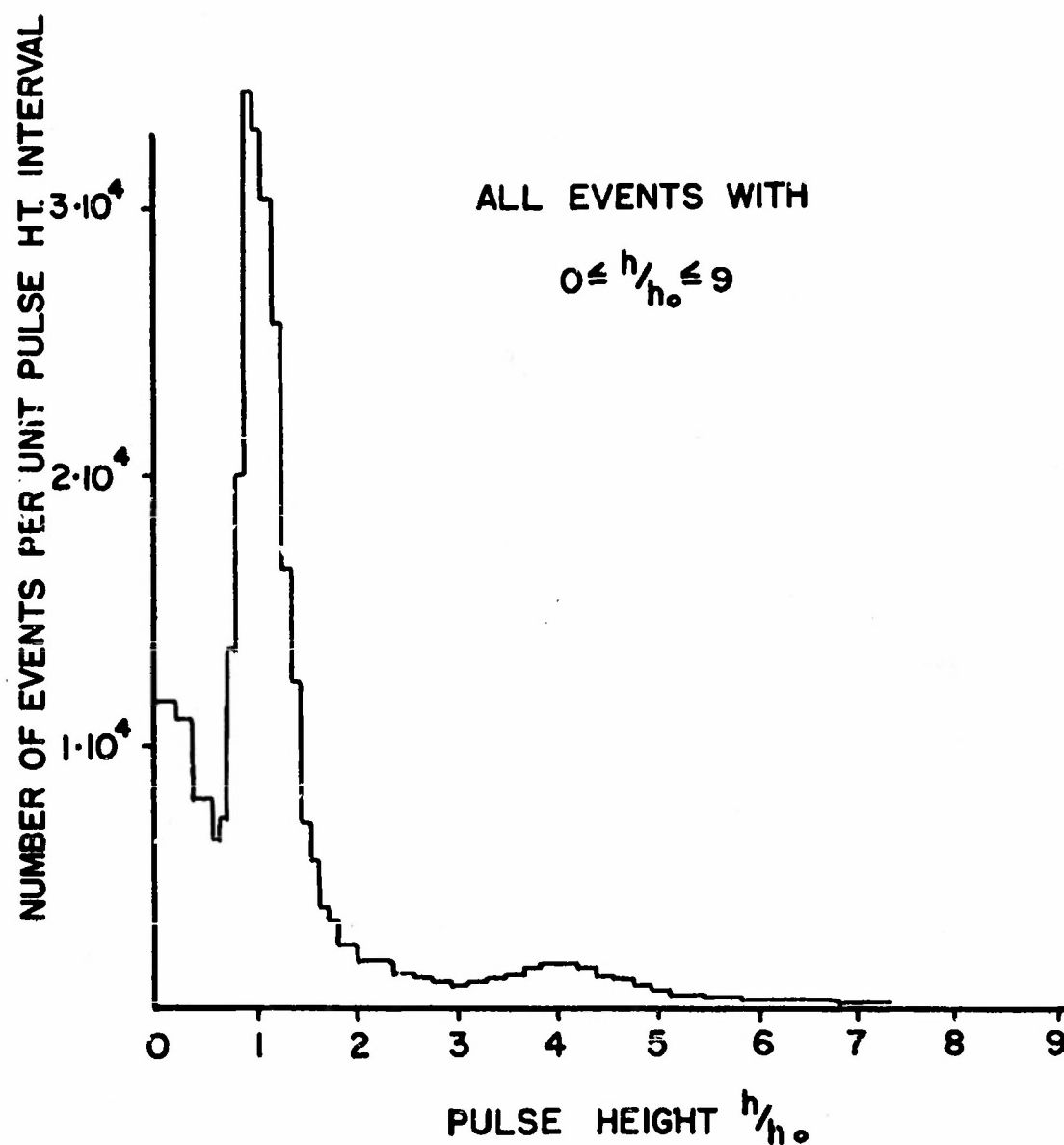
FIGURE 11.   Pulse height distribution for all events. This

distribution includes events in which the guard counters were

triggered and events in which more than one particle passed through
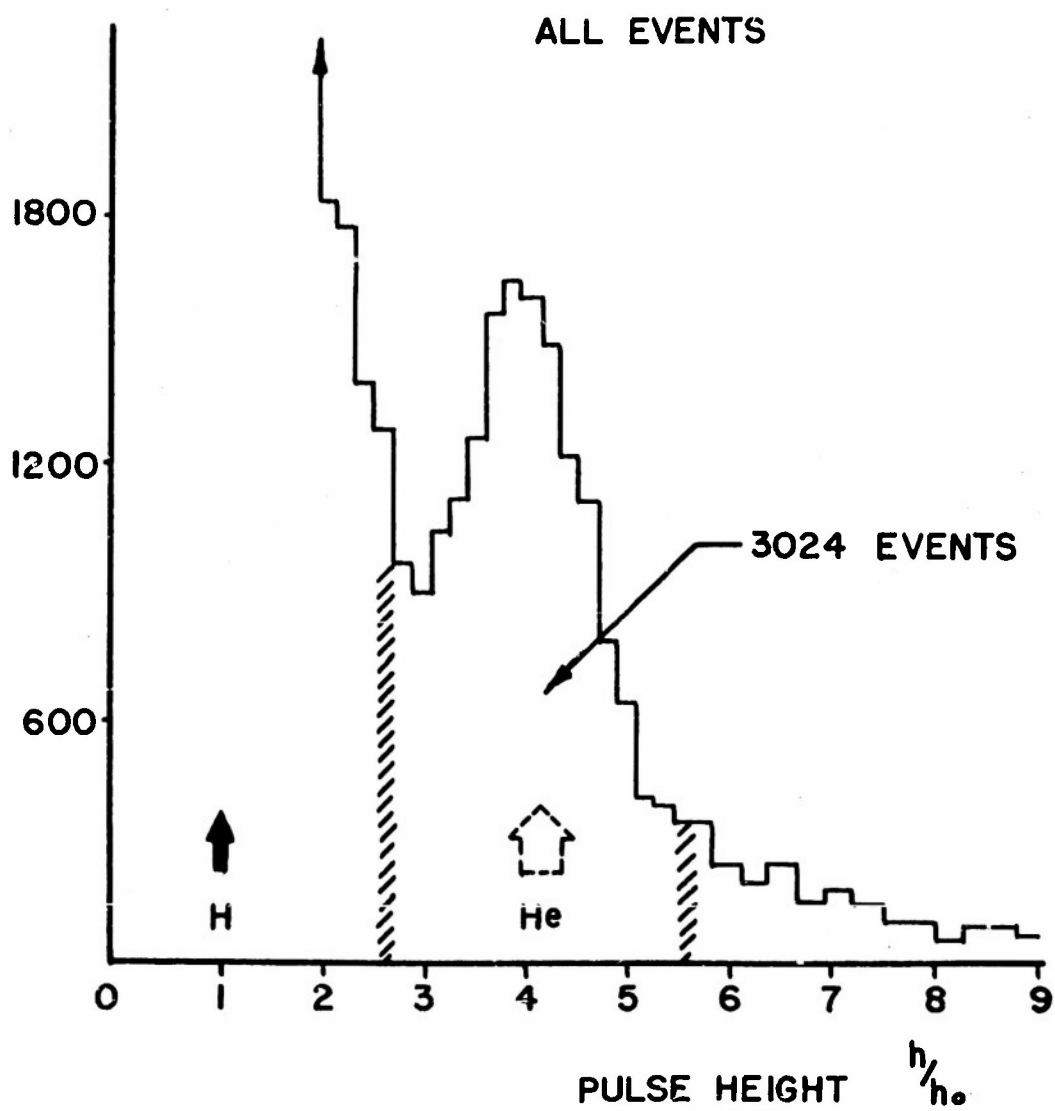
the detector.

FIGURE 12.   An enlarged view of the alpha region shown in
figure 11.

the curve between the two lines corresponds to 3024 events. The solid arrow was drawn under the proton peak, its width indicating the uncertainty in locating the peak. The dotted arrow was not centered under the alpha peak but rather was drawn at four times the pulse height corresponding to the proton peak. Its position can be compared to the observed position of the alpha peak.

Since all events are included in this pulse height distribution, the only discrimination involved is the inherent discrimination of a Cerenkov counter against slow particles. It is of interest to note that this, in itself, is enough to bring out a partially resolved alpha peak. Of course, many of the pulses in the alpha region are to be classed as background and, therefore, the next job is to try to determine which events are the true alphas.

It seems reasonable to say that all events in which the guard counters are triggered are not single alphas that passed vertically downward through the telescope. Therefore, these events are not what we are interested in and are to be classed as background (it was for this reason that the guard counters were included in the equipment). There is somewhat of a check on this assumption. If indeed the guard counter events are not associated in any way with alphas, their pulse height distribution should not show any structure in the alpha region. Figure 13 shows the pulse height distribution for the guard counter events only. Again the shaded lines define the region in which alphas are to be expected. Outside the lines there are no alphas, so all those pulses must be background. The distribution inside the shaded lines follows an interpolation of the curve outside. This is what you would expect if these events were all background as is being assumed. There are 451 guard counter events in the alpha region.

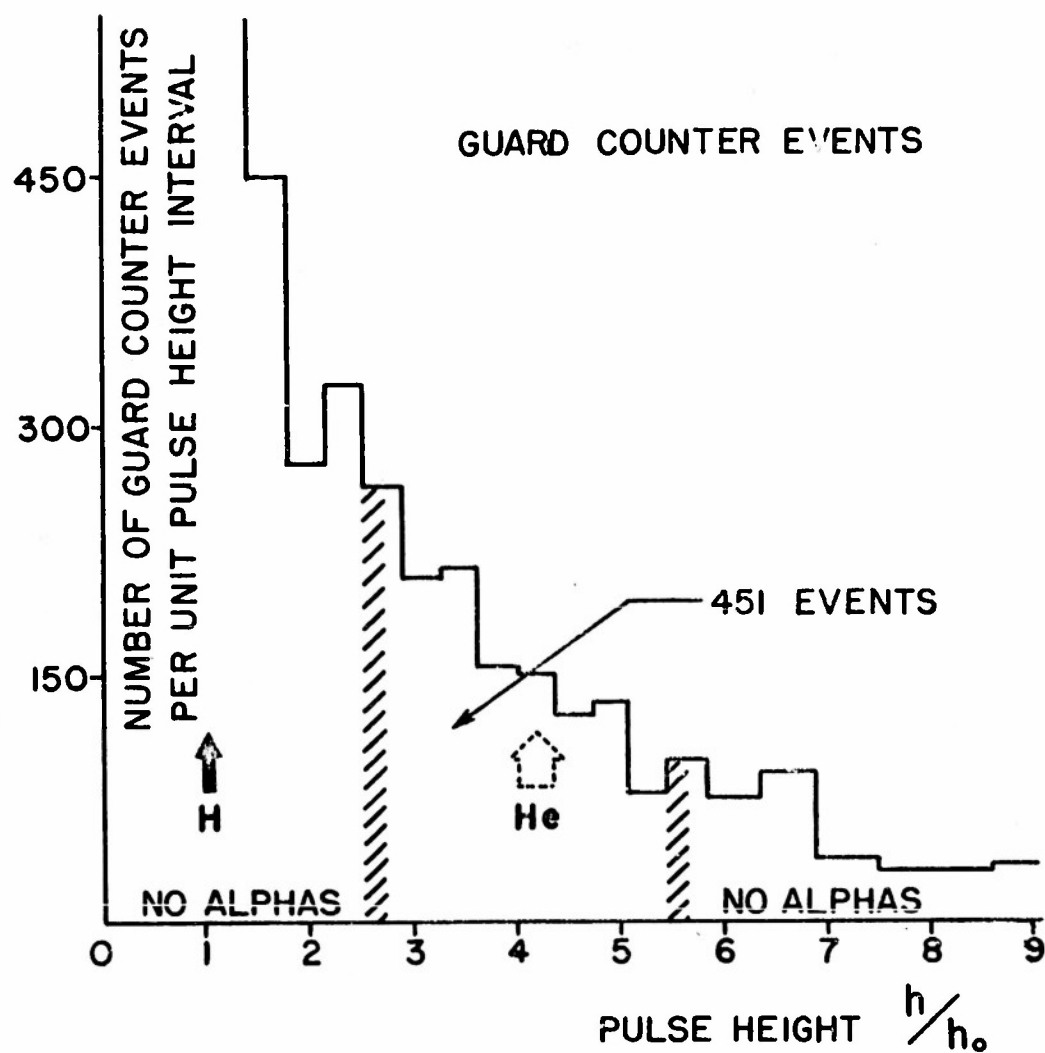Next consider the events in which more than one counter in trays

FIGURE 13. The pulse height distribution for events in which a guard counter was discharged. There is no "structure" in the alpha region, which is consistent with the assumption that all these events are background due to side showers.

B or C were triggered. As has been mentioned it was hoped that this device would identify background due to proton-induced nuclear interactions taking place in the lucite radiator. However, it is also possible for an alpha to cause more than one Geiger counter to be triggered simultaneously. This can come about in 3 ways. First, there is about 7 ± 3 gm/cm^2 of matter between the lucite and tray C. An alpha can go through the radiator, give a Cerenkov pulse of the right size, then interact in this matter and the resultant shower can trip more than one Geiger counter. Second, it is possible that a delta ray made by the alpha will trigger an additional Geiger counter, and third, a small number of alphas travelling at large angles will be able to pass through two adjacent counters. A crude estimate of these combined effects is worked out in appendix E. As is shown there, $18 \pm 9\%$ of all true alphas will trigger more than one Geiger counter in the bottom trays and therefore appear as a tipped pulse on the film. If this is the case then there should be a peak superimposed on the background of proton-induced interactions. Qualitatively this is what was found. Figure 14 shows the pulse height distribution for these multiple events. Again the shaded lines indicate the region in which alphas are expected. It is comforting that a small peak does appear and it does lie roughly within the shaded lines. Outside the shaded lines there should be no alphas. It must all be background. Therefore to get the background in the alpha region an interpolation was made and is indicated by the dotted line. The area under the peak but above the dotted line represents true alphas and amounts to 247 events. This is 17% of the number of events which were finally believed to be alphas. The area under the dotted line represents background and amounts to 651 events.

The pulse height distribution for what remained after using these two devices to identify background events is shown in figure 15. These

FIGURE 14. The pulse height distribution for events in which
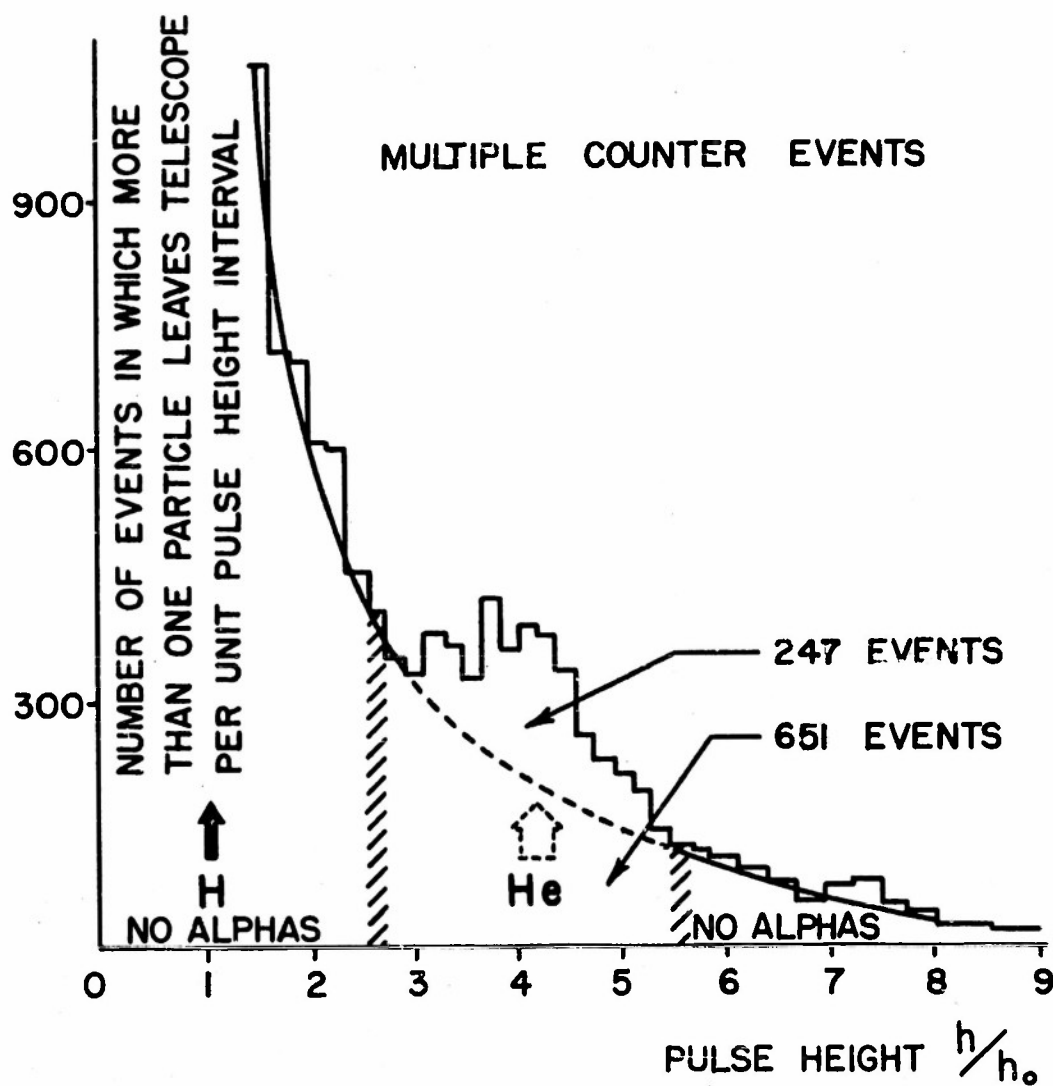two or more counters in tray B or C are triggered simultaneously.
Here there is "structure" in the alpha region. 247 events are
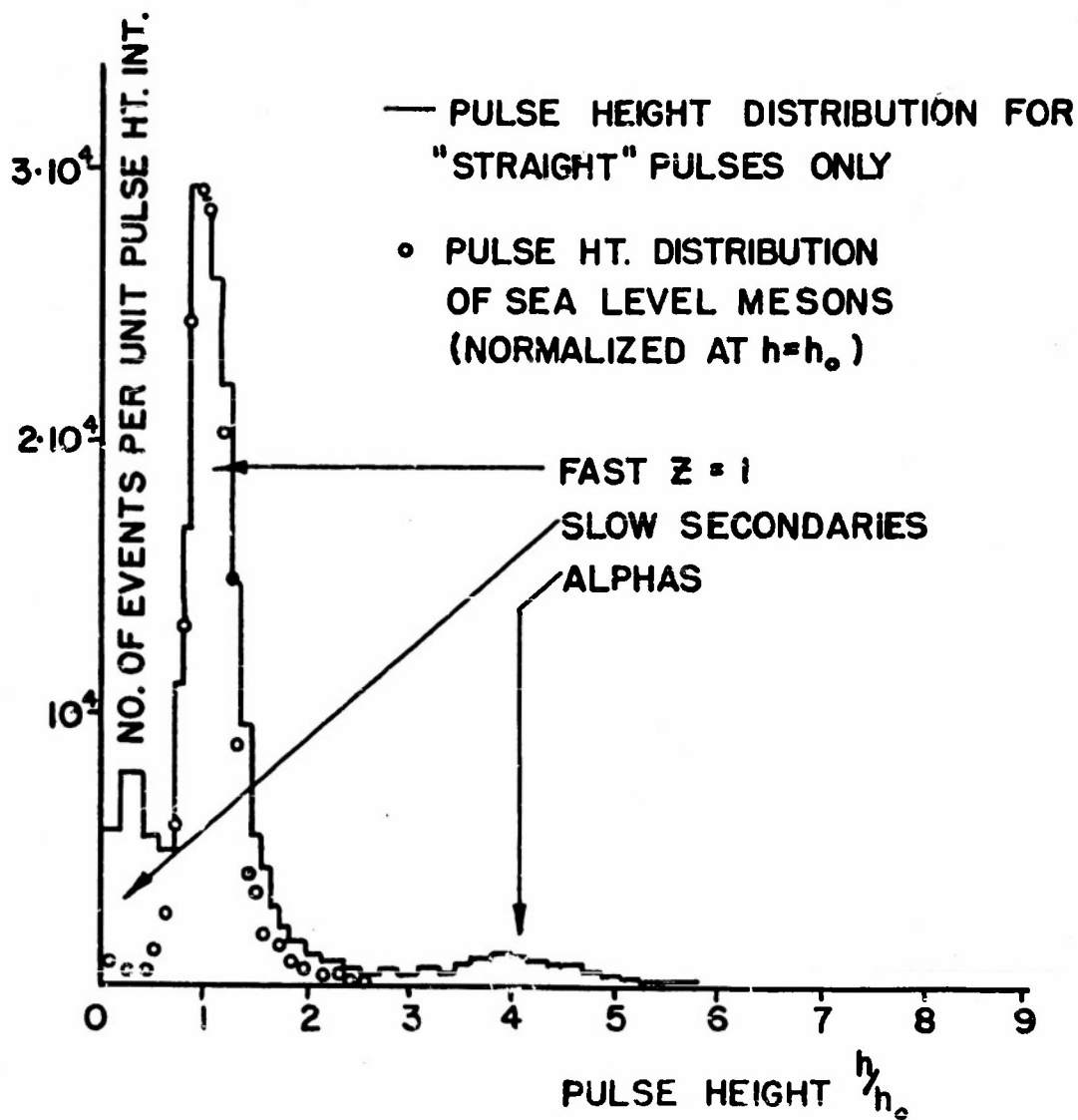due to alphas and 651 are due to proton-induced interactions.

FIGURE 15.   The pulse height distribution for "straight"
pulses only.   Events in which guard counters or multiple
counters in trays B or C were triggered are _not_ included.

are the pulses which appeared "straight" on the film. The dotted
curve is the pulse height distribution obtained from sea level mesons,
and it is therefore what one would expect to get at altitude if there
were nothing but fast protons. There is not appreciable broadening
in the main proton peak but there is an extra group of small pulses
due to single slow secondaries. This group does not blot out the alpha
region because the pulses are small, but had this been a device which
measured ionization loss those particles would have given pulses on
the other side of the proton peak and that would have been very bad.
This, of course, is the principle advantage of the Cerenkov counter.

Figure 16 shows an enlarged view of the alpha region. Now as can
be seen the alpha peak is more clearly resolved, but since the valley
doesn't drop to zero there must still be background. This means the
other devices were not 100% efficient in detecting non-alpha events.
There are two kinds of background here. One is caused by the tail of
the proton peak. These pulses do not actually extend into the alpha
region but do contribute to the curve to the left of the alpha peak.
The other background is probably caused by nuclear interactions which
failed to trip two Geiger counters, and it would give pulses of all
different heights. To estimate the magnitude of this background in the
alpha region we would like to make an interpolation as was done before,
but before interpolating it is necessary to subtract out the proton tail.
This can be done because it has the same shape as the known meson tail.
After the protons are subtracted out it is assumed that the remaining
pulses outside the alpha region are all nuclear interactions. These are
shown in solid black in figure 17. It is this solid black curve which
is used to interpolate the background into the alpha region. This
interpolation is indicated by the heavy dotted line.

An alternative method of estimating the background is to use data
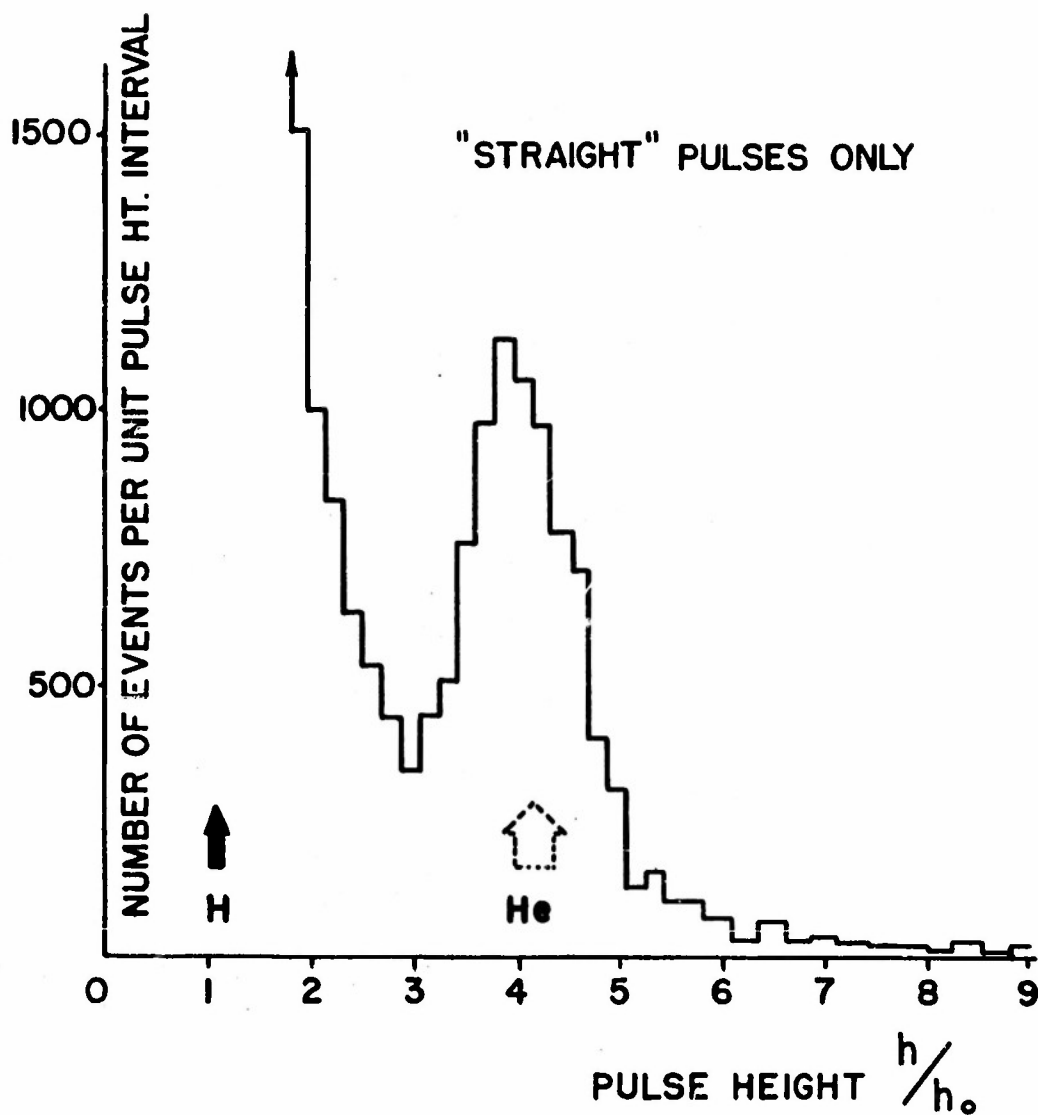
FIGURE 16. An enlarged view of the alpha region shown in figure 15.
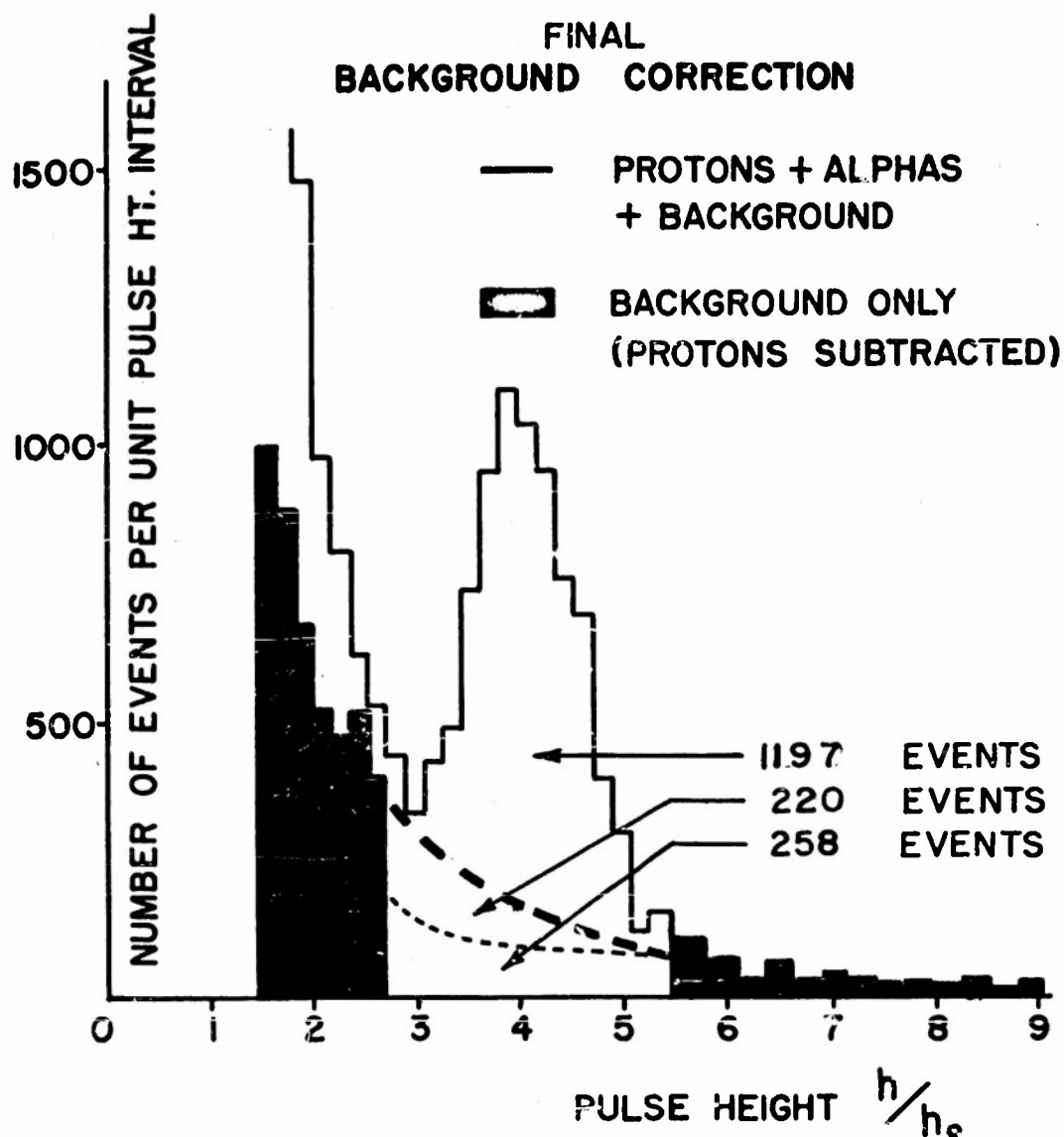
FIGURE 17.   The final background correction. The upper curve is a
repetition of figure 16. The solid black curve is what one obtains
after subtracting out the proton tail. The heavy dotted line is the
estimated background in the alpha region based on an interpolation of the
solid black curve. The light dotted line is the estimated background
based on data taken while the balloon was ascending.

obtained while the balloon is ascending. Here one takes the data
obtained at an altitude sufficiently high that there are appreciable
numbers of protons which can produce interactions, but sufficiently low
so that there are no alphas. Then all large pulses must be background.
Of course since we are dealing with protons which have been degraded in
energy, this may only give a lower limit for the background at altitude.
The background estimated in this way is shown by the lower dotted line.
This method has been used by various people in the past. Note that the
two methods, at least in the case of a Cerenkov counter, give significantly
different results.

The value obtained using the upper curve was taken as the estimated
background. This correction amounts to 478 particles which is 33% of the
total number of true alphas. This is a large correction and means there
is the possibility of a significant error in the result. This points up
the fact that in a counter experiment one must get a well resolved peak
if one hopes to get a precise value for the flux.

4.) The value of the alpha flux

After making this correction there are 1197 "straight" pulse events
remaining and it is assumed they are all true alphas. In addition there
were 247 multiple counter events which are believed to be alphas (page 34).
The time during which this total of 1444 events occurred is 355.5 ± 1
minutes. Using a mean free path of 50 gm/cm^2 for the absorption of alphas
in the 16 gm/cm^2 of air above the equipment and in the first cm of lucite
in the radiator, we finally obtain as the result of this experiment
the value (see equation 3 page 13)

$$f_v = \frac{(1444)}{e^{-17/50} \quad (355.5)(60) \quad (9.5 \ 10^{-4})}$$

$$= 99 \text{ particles/m}^2 - \text{steradian} - \text{second}$$

for the flux of alpha particles at the top of the atmosphere at a geomagnetic latitude of 41°.

The following is a list of factors which make this flux value uncertain:

	effect on alpha flux
statistical uncertainty in the number of observed alphas	± 3%
number of multiple counter events that were really alphas - correct to ± 25%	± 5%
value of the final background correction - correct to ± 30%	± 10%
value of the geometry factor - correct to ± 10%	± 10%
value of the mean free path for absorption of alphas in air - correct to ± 10%	± 3%
altitude - correct to ± 1 gm/cm^2	± 2%

These uncertainties are independent and therefore one is probably justified in adding them vectorially in order to estimate a net uncertainty in the flux value. This procedure results in an estimated uncertainty for the alpha flux of ± 16%. It should be noted that this is, to some extent, a subjective estimate.

Figure 18 shows the summary of alpha flux values that was given in figure 1 with three additions. The dot with the arrow next to it represents the result of this experiment. The two dots just below it represent the results of Bohl's[13] double scintillation counter and Linsley's[19] Cerenkov counter triggered cloud chamber. All three experiments were flown from Texas last February. As can be seen the three points are reasonably consistent and lie somewhat below the previous values. It would be very interesting now to have these experiments repeated at other latitudes in order to get a better idea of the
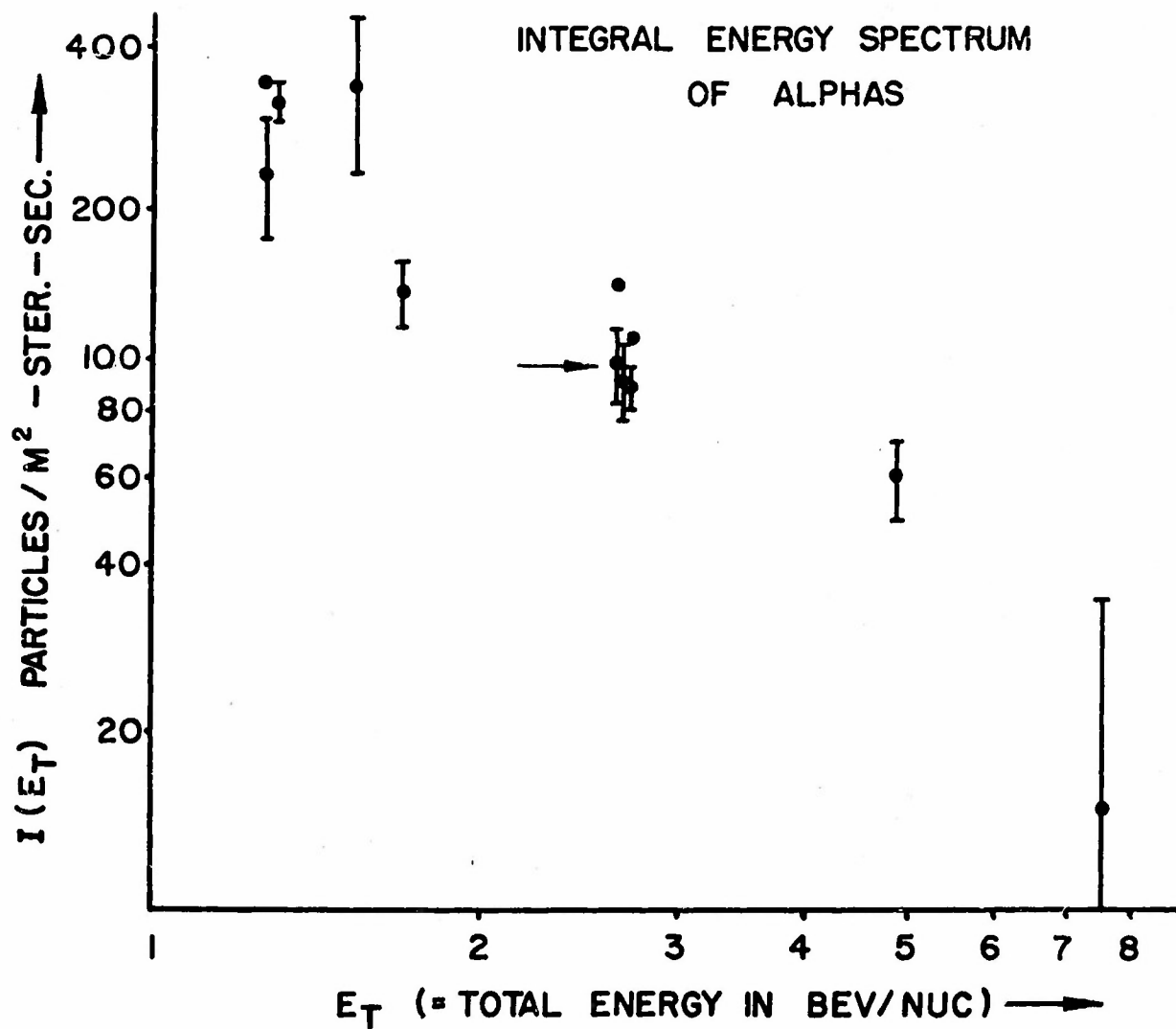
FIGURE 18. This is a repitition of Figure 1 except that three new points have been added at E_t = 2.75 Bev/nuc.. The point with the arrow is the result of this experiment. The two points just below it are due to Bohl and Linsley.

integral energy spectrum of primary alphas.

5) Time variations

The counting rate of all events was $1.38 \pm .01$ counts/sec. in the morning (9:30 to 12:30 c.s.t.) and $1.43 \pm .01$ counts/sec. in the afternoon (12:30 to 3:28 c.s.t.). This represents a 3.5% increase in the afternoon. The average geographic latitude, however, was 31° 6.1' in the morning and 31° 34.8' in the afternoon. This difference of approximately 29' changes the proton cut-off energy by about .16 Bev. Since $I_p(E_t) = K/E_t$ it follows that $dI/I = dE_t/E_t$ and with $dE_t = .16$ Bev and $E_t = 5.0$ Bev (the cut-off energy at 41°) we find that we should expect an increase in the afternoon of 3.2% due to the northward drift of the balloon.

We expect an effect of the same magnitude for the alpha flux (or slightly bigger if the energy spectrum is steeper). Actually the morning and afternoon counting rates were $2.65 \pm .12$ counts/sec. and $3.08 \pm .13$ counts/sec. respectively, which represents a 15% increase. The extra 12% is hardly significant since each value is only known to about 5%. Thus the data indicates that to within, say $\pm$ 20%, the alpha flux at 41° does not exhibit any time variation between morning and afternoon.

6) High total counting rate

The average counting rate for all events was 1.4 counts/sec. This represents a flux of 1450 particles/m^2-steradian-sec. Winckler[20] has reported a value of 1100 particles/m^2-steradian-sec. for the total flux at 40° at an atmospheric depth of 16 gm/cm^2 as measured by a large Geiger counter telescope with no additional absorber. Thus the Cerenkov counter has a total counting rate which is 30% higher.

All guard counter events and multiple counter events have been included in the figure 1.4 counts/sec. because Winckler's telescope

did not have any special devices to eliminate showers and interactions. On the other hand the Cerenkov counter contains more local matter than does the Geiger counter telescope and this may be what produces the extra counts. The lucite radiator is larger than the top Geiger counter tray and is located just below it. Thus protons may come in at large angles, interact in the lucite, and secondaries trip the bottom trays. If one subtracts out the events which trigger a guard counter or more than one Geiger counter, then the total counting rate is 1.04 counts/sec. which corresponds to 1090 particles/m^2-steradian-sec.

This effect is being mentioned for the sake of completeness. No attempt will be made to draw any quantitative conclusions.

7) Results at altitude in the region $10 \leq h/h_o \leq 80$

Figure 19 shows the pulse height distribution in the range $10 \leq h/h_o \leq 80$ for the events which give "straight" pulses (i.e. events which triggered a guard counter or more than one counter in trays B or C are not included). The regions of pulse heights which one expects to correspond to the various elements are indicated along the abscissa. These regions have been determined by using

1) The Z^2 dependence for Cerenkov light

2) The amplifier calibration curve (figure 22)

3) The fact that the peaks are smeared downward by 13% due to variations in the energy of the primaries (figure 23) and then smeared out symmetrically an additional few per cent due to other fluctuations.

The charge resolution is not outstanding; however, there is some indication of partially resolved carbon and oxygen peaks. In judging the usefulness of a Cerenkov counter in the CNO region on the basis of figure 19 one should remember that

1) The distribution involves rather few events (69 in the CNO

"STRAIGHT" PULSES ONLY
$9 \leq h/h_o \leq 80$
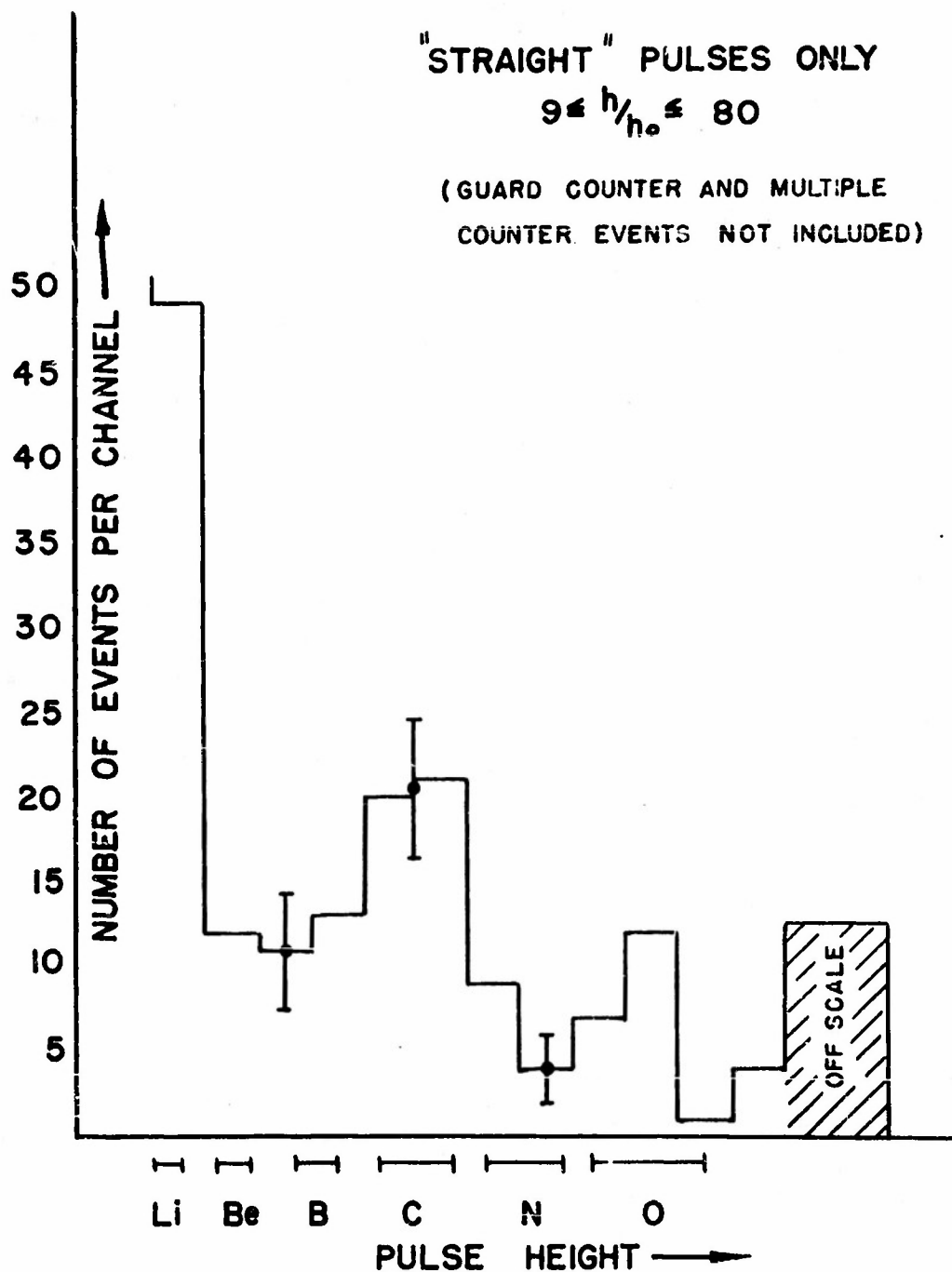
(GUARD COUNTER AND MULTIPLE
COUNTER EVENTS NOT INCLUDED)

FIGURE 19.

region) and this makes resolution difficult.

2) The effect of variations in energy spreads out the peaks to a serious extent. (One would be better off in this respect if the experiment were done at the equator.)

Next consider the pulse height distribution for all events (both straight and tipped pulses). This is shown in figure 20. During the 355.5 minutes at altitude there were 209 events which gave pulses in the CNO region. Of these, 25 triggered a guard counter, 115 triggered multiple counters in trays B or C, and the remaining 69 gave "straight" pulses. If one believes that proton-induced nuclear interactions will not give pulses in the CNO region when one uses a Cerenkov counter, then all 209 events must be associated with true CNO's. This is actually quite possible since CNO's have a large probability of making delta rays which could trigger a guard counter or a second Geiger counter. Extrapolating the total counting rate to the top of the atmosphere using a mean free path of 35 gm/cm^2 one obtains an upper limit for the CNO flux of 17 particles/m^2-steradian-sec. This is to be compared with the value 6 particles/m^2-steradian-sec. obtained with emulsions[12]. Thus, either there are background events that are not associated with CNO's or the geometry factor is 2 or 3 times bigger for CNO's than for protons. Linsley[19] has obtained results with his Cerenkov triggered cloud chamber which indicate the geometry factor is increased for CNO's. This happens because some CNO's which pass through the lucite but miss one of the trays of the telescope get recorded anyway because a delta ray triggers the missed tray.

It might be noted that including guard and multiple counter events (figure 20) caused considerable "fill-in" to the left of the carbon peak (thus contradicting the assumption that tipped pulses are simply CNO's accompanied by delta rays). This may be explained by saying
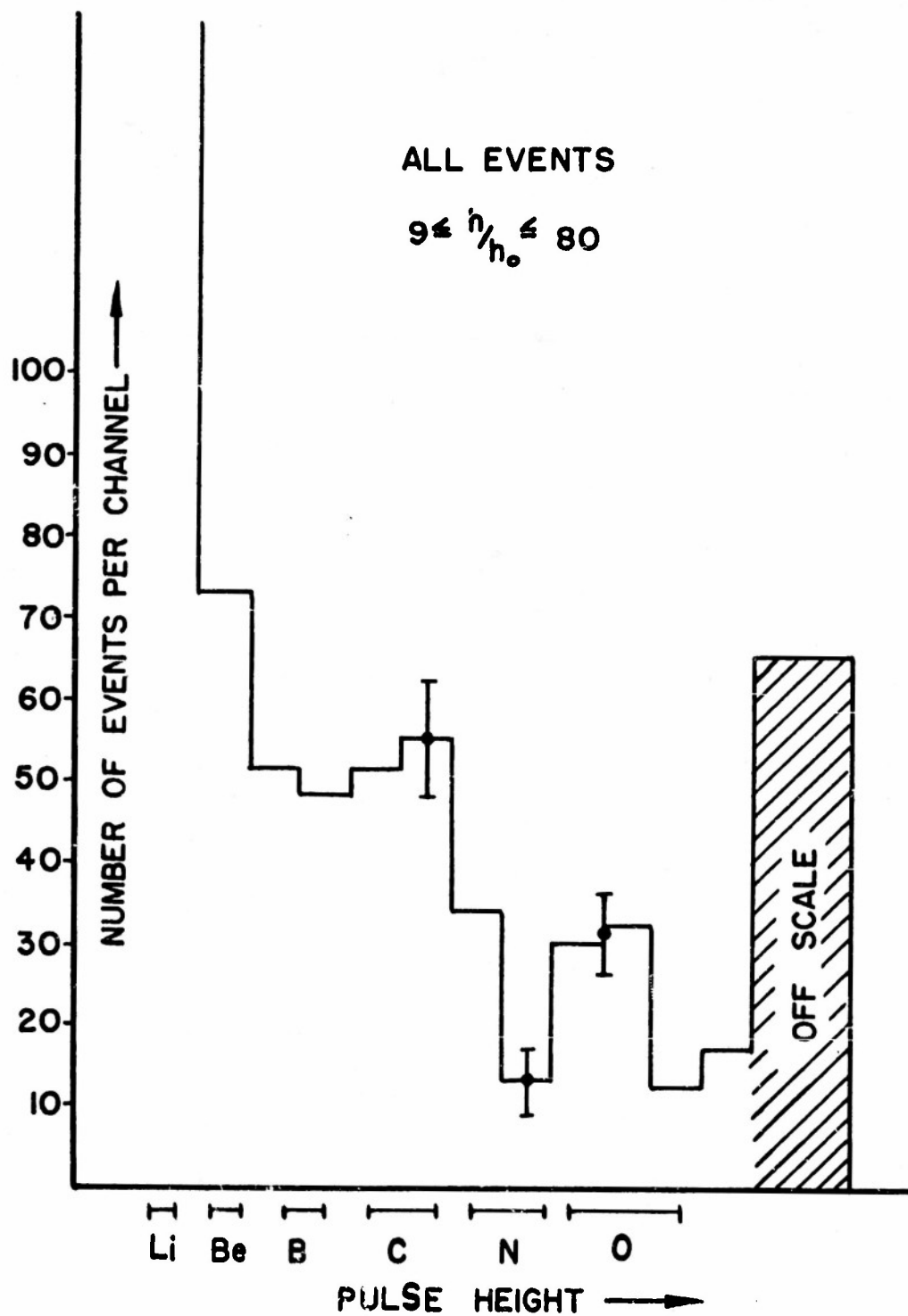
FIGURE 20.

1) The structure in both figures 19 and 20 is only fortuitous.

2) The "background" to the left of the carbon peak is proton
induced and not caused by actual carbon nuclei.

Finally consider the "off-scale" pulses. These correspond to $Z \geq 10$.
Some additional indication of the behavior of the Cerenkov counter and
the Geiger counter telescope can be obtained by comparing the number of
these events with the number of CNO events. Using only events which
give "straight" pulses and extrapolating to the top of the atmosphere
one finds $\frac{CNO}{Z \geq 10} = 2.1$. Taking all events and extrapolating to the
top of the atmosphere gives $\frac{CNO}{Z \geq 10} = 1.3$. Using emulsions, on the
other hand, one finds that the ratio of the flux of CNO to the flux of
$Z \geq 10$ is approximately 3.

This disagreement is qualitatively consistent with the picture that
all large pulses are due to heavies but that delta rays open up the
telescope and also cause multiple Geiger counters to be discharged.
Thus, since the number of delta rays goes as Z^2, the geometry factor
will be bigger for $Z \geq 10$ than it is for CNO's. This explains why
both observed ratios are less than 3. Similarly, a greater proportion
of $Z \geq 10$ events should trip multiple Geiger counters than will be the
case for CNO. events. This explains why the ratio for straight pulses
(2.1) was greater than the ratio for all events (1.3).

PART VII. CHANGES FOR FUTURE EXPERIMENTS

1) Eliminate ambiguity in left and right deflections

The amount of right or left deflection depended on how many guard
counters or Geiger counters in trays B or C fired simultaneously. It
is possible that right and left deflections partially cancelled each
other. There were a few cases in which it was hard to decide whether

a pulse was tipped or not. This made analyzing the data more time consuming and injected a subjective element into the results. This can be eliminated by making the two signals clearly different in shape.

It may be feasible to make use of the magnitude of the deflection, i.e. the size of the left deflection tells how many Geiger counters were triggered and thus puts a lower limit on the size of the shower (or the number of delta rays). No attempt was made to do this in this experiment.

2) Additional Geiger counter tray

A possible explanation for the large total flux is that particles pass through tray A from all directions, interact in the lucite, and a product of the interaction trips B and C. It is particularly bad to have condensed matter just under the top tray as was the case in this experiment. It might be worthwhile to have another large tray of thin wall counters located 6" above tray A.

3) Larger geometry factor

If this experiment were to be repeated at the equator the counting rate would probably be down by a factor of at least 3. One run was made on the ground in which tray A was doubled in size by simply adding two more Victoreen counters. The half-width of the meson curve remained the same (approximately 45%). There were not enough events to determine the effect on the size of the "tail", but it appears that the geometry factor can be increased by at least a factor of 2 with no trouble.

4) Smaller diameter Geiger counters in trays B and C

As was pointed out on page 37 the devices to detect background events were not 100% efficient. This led to the necessity of making a fairly large correction just on the basis of an interpolation (page 40). It may be worthwhile to improve the detection efficiency for

proton interaction events by using Geiger counters of smaller diameter
in tray B and C.

5) Blackening the lucite radiator

One may be able to use the directional properties of Cerenkov
light in discriminating against side showers. In lucite the photons
are emitted in a direction that makes a 48° angle with the direction
of the incident particle. The amount of light from a side shower
would be reduced by blackening the top and sides of the radiator, so
that light striking these surfaces would not be reflected into the
photocathode.

6) Attempt to achieve higher altitude

As one goes down in the atmosphere the flux of alphas decreases
but the flux of protons increases. This would be even more true at the
equator than it was at Texas, since the primary protons are more energetic.
Thus a high balloon flight would be a great help in eliminating back-
ground in the alpha region.

ACKNOWLEDGEMENTS

APPENDIX A. DETERMINATION OF THE GEOMETRY FACTOR

1) Outline of the method

Let G_{iso} be the geometry factor for an isotropic flux

G_{cos^2} be the geometry factor for a cos^2 flux

We wish to know G_{iso}. If we knew the effective lengths, efficiencies, etc. for each Geiger counter, we could make an exact calculation. Unfortunately, there is an uncertainty in these quantities and the apparatus is no longer available for experimental determinations. Nevertheless, it is estimated that both G_{iso} and G_{cos^2} can be calculated to $\pm$ 10%. Their ratio can probably be calculated to within a few percent. These calculations are given in section 2.

We can get an independent estimate of G_{cos^2} experimentally by measuring the counting rate of the telescope on the ground if we know the flux. This was done in the basement of the physics building where the counting rate was determined to a statistical accuracy of $\pm$ 3%. The flux was then measured using a large telescope where end corrections etc. were negligible. Unfortunately, there was an uncertainty in the measured flux due to showers which amounted to $\pm$ 10%. The geometry factor for a cos^2 distribution determined in this way is given in section 3.

An additional piece of information is the counting rate observed inside a wooden building at San Angelo, Texas. Again the counting rate was known to $\pm$ 3%. The flux was deduced from the work of others reported in the literature with appropriate corrections estimated for absorption in the building, etc. These are large corrections which are difficult to estimate, so although this information was used it was given relatively little weight.

The values of $G_{\cos 2}$ were averaged and this best value plus the calculated ratio $G_{iso}/G_{\cos 2}$ was used to get a best value for G_{iso}.

2) Direct calculation

The aperture of the telescope is defined by trays A and C. If the linear dimensions of each of these trays were small compared to the distance between trays, one could use the approximate expression

(equation 5) $$G_{iso} = A_a A_c / h^2$$

where:

A_a is the area of tray A

A_c is the area of tray C

h is the distance between trays

This is a "point-point" approximation (both finite areas being approximated by points). In the Cerenkov counter telescope the dimensions are as follows:

tray A $\quad$ 3/4" x 2-3/4"

tray B $\quad$ 8" x 8"

h $\quad$ 12"

Whereas the dimensions of tray A are small compared to h, this is not true of tray C. Therefore, in calculating the geometry factor, a "point-rectangle" approximation was used, i.e. the small upper tray was approximated by a point but no approximation was used in regard to the lower tray. Figure 21 illustrates the approximation, and defines the angles $\bar{\theta}$, $\bar{\varphi}$, θ, φ and the dimensions L and D. $\bar{\theta}$ and $\bar{\varphi}$ are the usual zenith and azimuthal angles in spherical coordinates but for the point-rectangle problem the new variables θ and φ are more convenient.

Let:

$f(\bar{\theta})$ $\quad$ be the flux of cosmic rays

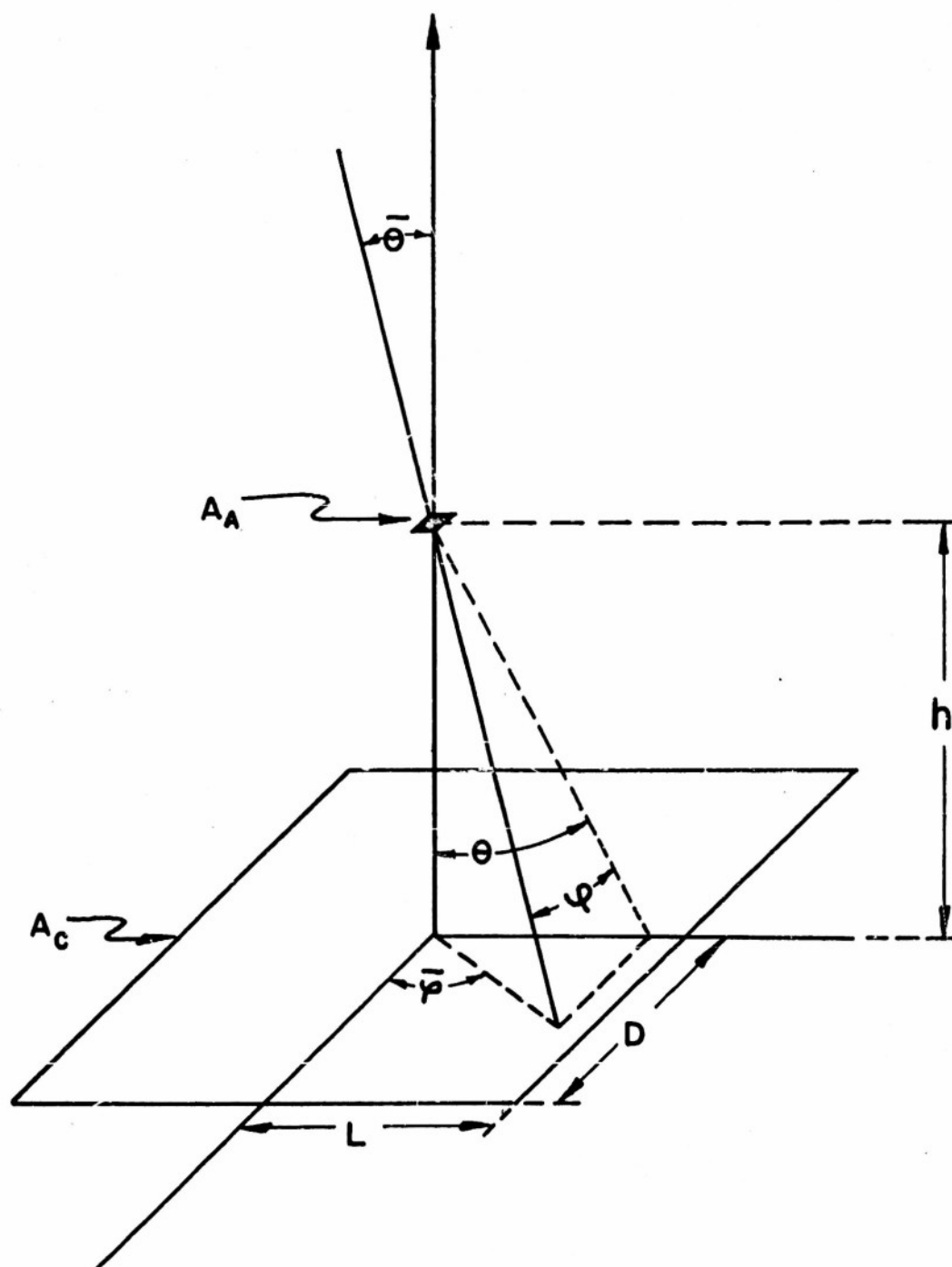N $\quad$ be the rate at which cosmic rays pass through the telescope

FIGURE 21.   The "point-rectangle" approximation. $\bar{\theta}$ and $\bar{\varphi}$
are the usual zenith and azimuthal angles in spherical coordinates.
The new angles θ and φ are more convenient for this problem.

dN   be the rate at which cosmic rays pass through the telescope

coming from the allowed direction $\bar{\theta}$ to $\bar{\theta} + d\bar{\theta}$; $\bar{\varphi}$ to $\bar{\varphi} + d\bar{\varphi}$

At the top of the atmosphere the flux is isotropic; therefore, $f(\bar{\theta}) = f_v$,

and

$$dN = (f_v)(A_a \cos\bar{\theta})(\sin\bar{\theta} \ d\bar{\theta} \ d\bar{\varphi})$$

$$= (f_v)(A_a \cos\theta \cos\varphi)(\cos\varphi \ d\theta \ d\varphi)$$

$$N = 4 \ f_v \ A_a \int_0^{\tan^{-1}\frac{L}{h}} \cos\theta \ d\theta \int_0^{\tan^{-1}\frac{D\cos\theta}{h}} \cos^2\varphi \ d\varphi$$

The integration is straightforward. Introducing the dimensionless variables $a \equiv D/h$ and $b \equiv L/h$ one obtains:

(equation 6) $N = f_v \left\{ 2A_a \left[\frac{b}{\sqrt{1+b^2}} \ \tan^{-1}\left(\frac{a}{\sqrt{1+b^2}} \right) + \frac{a}{\sqrt{1+a^2}} \ \tan^{-1}\left(\frac{b}{\sqrt{1+a^2}} \right) \right] \right\}$

$$= f_v \left\{ G_{iso} \right\}$$

If we are dealing with the flux on the ground, then $f(\bar{\theta}) = f_v \cos^2\bar{\theta}$

In this case

$$N = 4 \ f_v \ A_a \int_0^{\tan^{-1}\frac{L}{h}} \cos^3\theta \ d\theta \int_0^{\tan^{-1}\frac{D\cos\theta}{h}} \cos^4\varphi \ d\varphi$$

(equation 7) $N =$

$$f_v \left\{ \frac{A_a}{2} \left[\frac{(3+2a^2)a \ \tan^{-1}\sqrt{\frac{b}{1+a^2}}}{(1+a^2)^{3/2}} + \frac{(3+2b^2)b \ \tan^{-1}\sqrt{\frac{a}{1+b^2}}}{(1+b^2)^{3/2}} - \frac{ab(2+a^2+b^2)}{(1+b^2)(1+a^2)(1+a^2+b^2)} \right] \right\}$$

$$= f_v \left\{ G_{\cos 2} \right\}$$

The quantities in curly brackets are the expressions for the geometry factors. For the Cerenkov counter telescope:

$A_a = 4.07$ in^2 $\pm 7\%$

$L = 4.00$ in $\pm 3\%$ } based on quoted active lengths

$D = 3.82$ in $\pm 0.5\%$

$h = 11.9$ in $\pm 1\%$

This leads to $\quad G'_{iso} = 9.75$ cm^2 – steradian

$$G'_{\cos 2} = 9.16 \text{ cm}^2 - \text{steradian}$$

The Gs are primed because there are a number of corrections which must be applied. These are as follows:

1) dead space in tray B due to finite wall thickness of counters

2) end corrections for tray A and tray C (mathematically, the trays were approximated by plane surfaces with no thickness).

3) effective length corrections for tray A and tray C (there is reason to believe the effective lengths are not quite equal to the quoted active lengths).

4) efficiency corrections for trays A, B, and C (in the calculation these efficiencies were assumed to be 100%).

The combined effect of these corrections amounts to a $5\% \pm 5\%$ reduction in the geometry factors. The results we will use are:

$$G_{\cos 2} = 8.7 \text{ cm}^2 - \text{steradian} \pm 10\%$$

$$G_{iso}/G_{\cos 2} = 1.07$$

3) Value of $G_{\cos 2}$ as determined experimentally at Minneapolis

A telescope similar to that used by Montgomery[21] was used to measure the flux in the sub-basement of the Physics Building at the University of Minnesota. The important point is that the Geiger counters were long so that uncertainties in effective length and end corrections were small.

(In addition, transverse counters were used in an attempt to eliminate
the uncertainty altogether.) This standard telescope contained approxi-
mately 8 gm/cm^2 of matter, which is approximately the same as the amount
of matter in the Cerenkov telescope. Let:

G_s be the calculated geometry factor of this "standard" telescope

N_s be the counting rate of this "standard" telescope

N be the counting rate of the Cerenkov counter telescope

then:

(equation 8) $G_{cos2} / G_s = N / N_s$

G_s can be calculated to within a few percent, and the statistical un-
certainty in N_s and N can be made negligible. Thus, this method looks
capable of yielding a precise value for G_{cos2}. Unfortunately, there
seems to be a significant number of shower events in the sub-basement,
and the detection efficiency for these events is higher for the standard
telescope than for the Cerenkov counter telescope. Of course, in
equation 8 the Ns refer to the counting rate of single particles.

The standard telescope had a geometry factor of 11.5 cm^2 - steradian
$\pm$ 2% for a cos^2 flux, and the counting rate at one particular location
was 6.15 counts/min. $\pm$ 2%. It was estimated that 10 $\pm$ 6% of these events
were due to showers. At the same location N was observed to be 4.12
counts/min. $\pm$ 3%. Using these values, equation 8 yields

$$G_{cos2} = 8.5 \pm .9 \ cm^2 - \text{steradian}$$

4) The value of G_{cos2} using observed counting rate at San Angelo

The counting rate at San Angelo was measured to a statistical
uncertainty of $\pm$ 3%. The flux at San Angelo was estimated using
Montgomery's[21] value for the sea level flux and then applying corrections
for the altitude at San Angelo, absorption in the building at San Angelo,

and absorption in the Cerenkov counter telescope. This procedure led to the value $G_{cos2} = 11 \pm 2$ cm^2 - steradian.

The corrections which must be made are so large and uncertain that it was not felt this method should be given equal weight with the other two. Somewhat arbitrarily, the value 11 was given a weight of .3 and averaged with the other values 8.5 and 8.7 to obtain $\overline{G}_{cos^2} = 8.9 \pm 1$ cm^2 - steradian. Using the calculated G_{iso}/G_{cos^2} ratio we finally obtain

$$\overline{G}_{iso} = 9.5 \pm 1 \text{ cm}^2 - \text{steradian}$$

APPENDIX B.   TEST TO SHOW THAT THE DUMONT PHOTOMULTIPLIER IS INSENSITIVE TO THE EARTH'S MAGNETIC FIELD

A NaI crystal was coupled to the cathode of the photomultiplier. Then a Cs source was brought near and the output was displayed on an oscilloscope. A fairly well-defined photoelectric line was observed. The size of these pulses is proportional to the photomultiplier gain.

A magnet was then brought sufficiently near so that its movement would cause a compass needle located at the photomultiplier to make complete revolutions. At no time was there any visible variation in the pulse height corresponding to the photoelectric line.

APPENDIX C.   CALIBRATION OF AMPLIFIERS AND OSCILLOSCOPES

When a particle passes through the detector we desire to know the relative amount of Cerenkov light that it produces in the lucite. We assume the voltage output of the photomultiplier is proportional to this amount of light. We would hope that the height of the pulse recorded on the cathode ray tube is proportional to the voltage output of the photo-

multiplier, and it is to a first approximation. However, there is some saturation for large signals, and this saturation requires that we make a calibration.

A unit was built to produce artificial pulses which could be fed into the system at the 10th dynode connection. (This is where the signal was taken off the photomultiplier.) The pulse generator contained a low impedance, variable attenuator made of non-inductive, precision ($\pm$ 1%) resistors. Thus the size of the signal fed into the amplifier system could be varied in a precise way. The outputs from the amplifiers were fed to the two cathode ray tubes which in turn were photographed. The measured pulse heights were compared with the relative size of the input signals and thus both amplifiers and cathode ray tubes were calibrated. This was done just before the actual flight and the results are shown in figure 22.

APPENDIX D.   CRUDE PREDICTION OF THE SHAPE OF THE ALPHA PEAK

We wish to get a rough idea of the shape of the alpha peak taking into account fluctuations in the number of photoelectrons and variations in the energy of the incident alpha (what we will really use is the knowledge of the region in which there are no alphas).

First we consider the effect of variations in the energy of the alphas. Let:

L   be the amount of Cerenkov light emitted by an alpha of energy E expressed as a fraction of the saturation value.

i. e. $L = N(\beta)/N(1)$

R(L)   be the fractional number of events in which the amount of Cerenkov light lies between L and L + dL. (We desire an expression for $R(L)$.)
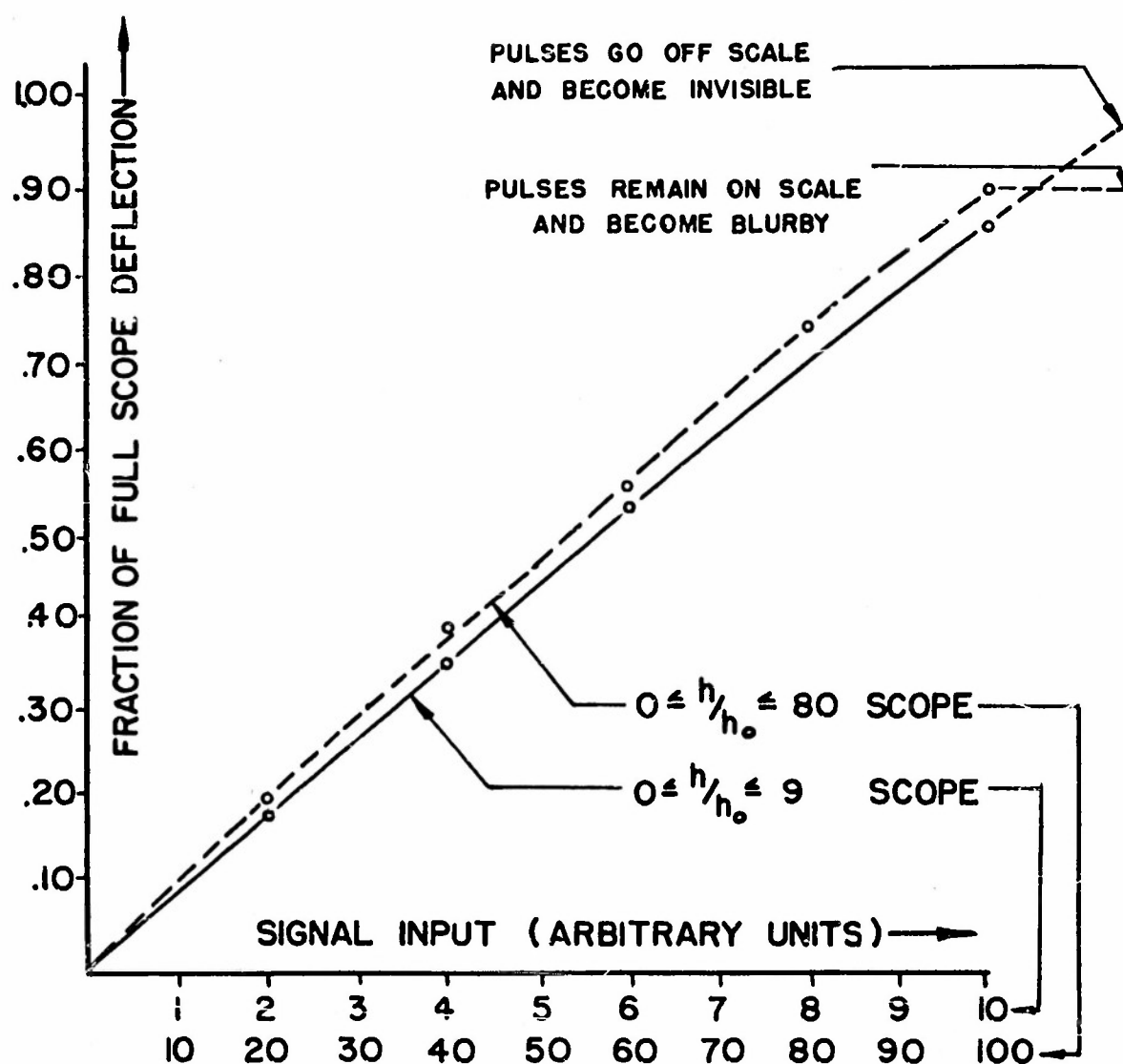
CALIBRATION OF AMPLIFIERS
AND CATHODE RAY TUBES

FIGURE 22.

$D(\gamma)$ be the differential energy spectrum for the alphas where

γ = total energy/rest energy

$\gamma = g(L)$ relate the amount of Cerenkov light radiated and the particle's

energy.

Then:

(equation 9) $R(L)dL = D\left[g(L)\right] g'(L)dL$

The function $\gamma = g(L)$ is obtained directly from equation 2 and the relation $\gamma = 1/(1-\beta^2)^{1/2}$ with the result:

(equation 10) $\gamma = \sqrt{\dfrac{n^2 + \dfrac{L}{1-L}}{n^2 - 1}}$

For the purpose of this calculation assume an integral energy spectrum $I(E_t) = K/E_t^{1.4}$ with a cut-off at $E_t = 2.7$ Bev/nuc. This leads to:

$$D(\gamma) = 0 \qquad \gamma \leqslant 2.7$$

$$= \frac{5.06}{\gamma^{2.4}} \qquad \gamma > 2.7$$

Calculating $d\gamma/dL$ from equation 10 and substituting into equation 9, we obtain:

(equation 11) $R(L) = \dfrac{2.5}{(1-L)^2 \left\{ \dfrac{L^2 + \dfrac{L}{1-L}}{n^2-1} \right\}^{1.7}} \qquad .85 < L < 1$

$$= 0 \qquad\qquad\qquad \text{otherwise}$$

This has been plotted in figure 23. It should be noted that the peak occurs near $L = 1$. Since the differential energy spectrum has its maxi-
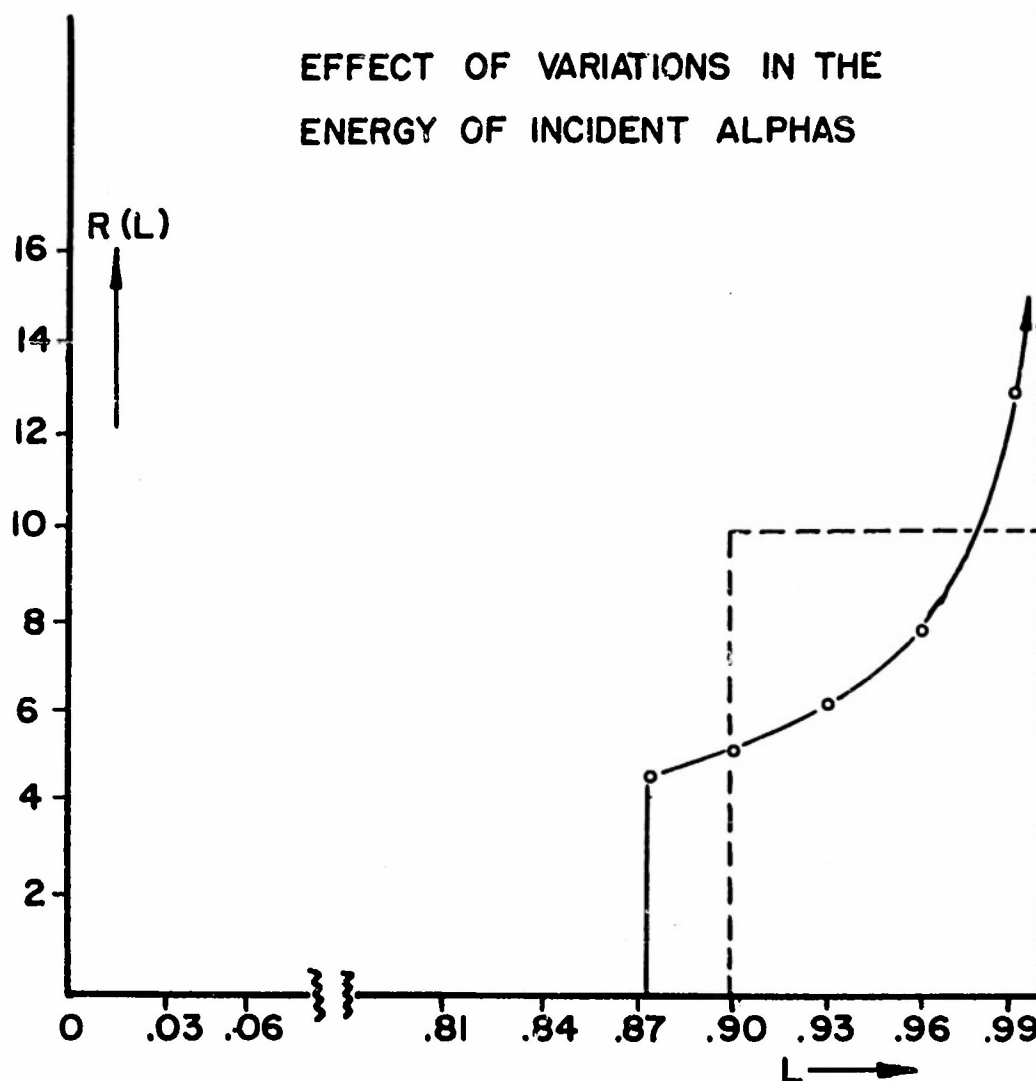
62

EFFECT OF VARIATIONS IN THE
ENERGY OF INCIDENT ALPHAS

FIGURE 23.   R(L)dL is the probability that an alpha which
enters the equipment at 41° will give an amount of light
between L and L+dL.   (L is in units of the saturation value.)
This curve gives the shape we would expect the alpha peak to
have if there were no fluctuations other than in the energy
of the primary alphas.   For purposes of calculation it has
been approximated by the dotted curve.

mum at the low energy end, one might think that $\bar{R}(L)$ would have its maximum value at the low end also. This is not the case because although the "density" of particles in "energy space" decreases at larger energies, still there are more high energy cosmic rays than low energy ones, and high energy cosmic rays all give values of L approximately equal to 1. If there were no other fluctuations, figure 23 would give the shape of the alpha peak.

Now we wish to combine the effect of variations in the amount of Cerenkov light produced with the effect of fluctuations in the number of photoelectrons produced. This could be done precisely but all that is desired (or warranted by the data) is a rough idea of the region of pulse heights in which the alphas will lie. Therefore, rather crude approximations will be made. The distribution of pulse heights due to fluctuations in the number of photoelectrons has been approximated by a Poisson distribution with mean .95(120) = 114. This distribution has a half-width of 22%. The distribution of pulse heights due to variations in energy alone (figure 23) was approximated by a square wave of width 10%. To combine the two effects, the Poisson distribution was simply "spread out" by 10%. This is crude and gives a resultant distribution which is too broad. Thus we obtain an upper limit for the size of the region in which the alphas will lie. After renormalizing this "spread out" distribution, it is found that all but a fraction of one percent of the alphas will have pulse heights $2.7 \leq h/h_o \leq 5.4$.

This result is open to question on the following grounds: The pulse height distribution for mesons shows a "tail" whereas the Poisson distribution drops off relatively fast. The meson tail (which includes about 4% of all meson events) is presumably due to events in which a knock-on electron is produced in the lucite with enough energy to emit Cerenkov light. Less than 4% of the alphas should lie beyond $h = 5.4\ h_o$,

however, because we are less likely to get an alpha accompanied by 4 simultaneous knock-ons than a meson with one knock-on.

APPENDIX E. ESTIMATE OF THE FRACTION OF ALPHAS WHICH WILL CAUSE MORE THAN ONE GEIGER COUNTER TO BE DISCHARGED

There are three effects: interactions, delta rays, and adjacent counters.

Interactions

Between the lucite and tray C there is 7 ± 3 gm/cm^2 of matter (photomultiplier, pre-amplifier chassis, Geiger counters). Assuming a collision mean free path of 50 gm/cm^2 we expect $14 \pm 6\%$ of the alphas to interact after traversing the lucite but before leaving the telescope. The next question is what fraction of these interactions will trigger more than one Geiger counter. An estimate can be made on the basis of data obtained while the balloon was ascending. At altitudes of 480 to 165 mb there are no alphas, so all large pulses must have been due to proton interactions in the lucite, and showers. 50% of these large-pulse events caused more than one Geiger counter to be triggered. Assuming roughly the same detection efficiency for alpha-induced interactions occurring below the lucite, we conclude that $7 \pm 7\%$ of the alphas will produce interactions which trigger 2 or more Geiger counters.

Delta rays

Let E be the energy an electron needs to penetrate a Geiger counter. Assume that when a particle of charge Z passes through matter exactly N_z delta rays with energy $\geq$ E leave the matter with the particle. (The matter is assumed thick enough so that equilibrium is established.) Then $N_z = Z^2 N_1$

Let   p   be the probability that a particular delta ray triggers

a Geiger counter other than that triggered by the parent

particle

P(k) be the probability that exactly k out of the N_z delta rays

trigger a second Geiger counter

Then:

P(0) = the probability that none of the delta rays triggers

a second Geiger counter

1 - P(0) = the probability that at least one delta ray will trigger

a second Geiger counter. This is the quantity we wish to

evaluate since we want to know what fraction of true alphas

will give tipped pulses because a delta ray triggered a

second Geiger counter.

We can estimate the value of this quantity for Z = 2 in the following

way: Since a delta ray either does or does not trigger a second Geiger

counter and since they are independent we know immediately that P(k)

is binomially distributed (page 26). Therefore,

(equation 12) $P(0) = (1 - p)^{N_1 Z^2}$

Thus, log P(0) vs Z^2 should be a straight line. We have that

P(0) = 1 for Z = 0. Next we will use the data in the CNO region to

estimate P(0) for Z = 6, 7, and 8. This will determine (to a first

approximation) the value of P(0) for Z = 2.

It seems unlikely that the multiple counter events which give

pulses in the CNO region are due to proton-induced interactions, as

this would require showers of 36 to 64 fast mesons occurring near the

top of the lucite. It has, therefore, been assumed that all multiple

counter events in the CNO region are due to true CNOs accompanied by

delta rays, or CNOs which interacted in the matter beneath the lucite.

Let:

s   be the number of events in which the pulse appears straight

t   be the number of events in which the pulse appears tipped to

        the left (because more than one Geiger counter has been triggered

        in trays B or C)

λ be the interaction mean free path for particles of charge Z

Then $(s + t)(1 - e^{-7/\lambda})$ is the number of particles which pass through

the telescope without interacting and

(equation 13) $$P(0) = \frac{s}{(s + t)(1 - e^{-7/\lambda})}$$

Values for s and t can be taken directly from the data. The values of

P(0) calculated in this way for Z = 4, 5, 6, 7, 8, and Z $\geq$ 10 are plotted

in figure 24. (Of course, we cannot use equation 13 to evaluate P(0)

for Z = 2 directly, because there is little hope that the assumption

on which it is based will be valid until we get out into the CNO region.)

The value of P(0) for Z = 2 is determined accurately enough from this

graph for our purposes in spite of the crudeness of the data. The two

lines represent extreme values of .89 and .96. Thus $8 \pm 4\%$ of alphas

will have delta rays that trip a second Geiger counter.

(The fact that P(0) for Be and B lies below the curve probably

means that many of the multiple events were not due to delta rays, as

was assumed, but were due to proton-induced interactions. On the other

hand, it is not clear why P(0) for the off-scale pulses tends to be

high.)

(A delta ray needs about 1 Mev to get into a Geiger counter. It

has been reported[22] that N_1 is about .07. Using this value, we can

evaluate p, the probability that a particular delta ray triggers a

Geiger counter other than that triggered by the parent particle. The

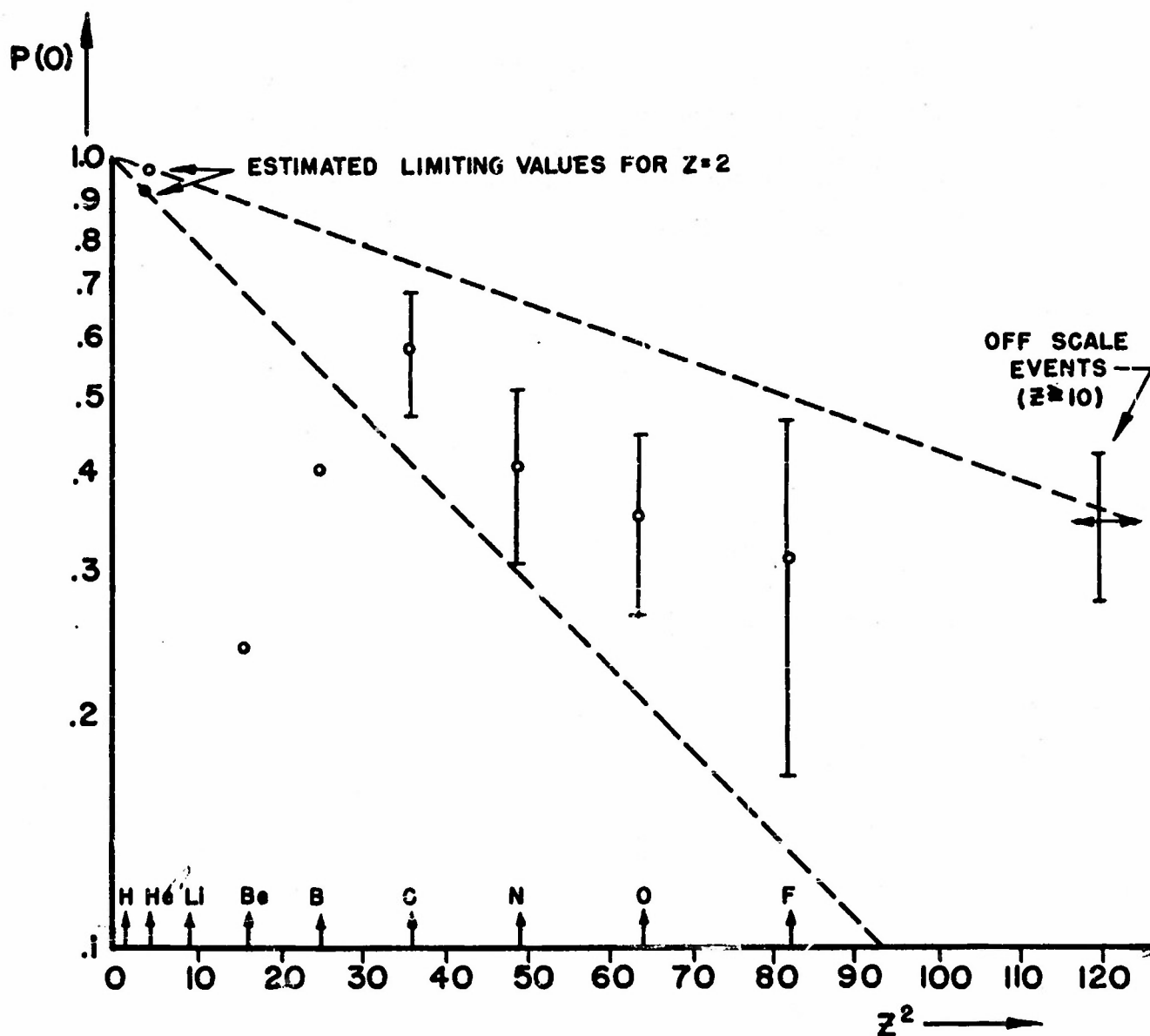result is: p = 1/4. p is the "probability of detecting a delta ray."

FIGURE 24.   P(O) vs Z^2

P(O) is the probability that a particle of charge Z passes through

the detector without making a delta ray that triggers a second Geiger

counter. We expect that   log P(O) vs Z^2 will be a straight line.

Since P(O) = 1 for Z = 0 we can get an estimate of P(O) for alphas from

data in the CNO region. The error bars represent statistical errors only.

In calculating the interaction effect, we assumed the probability that an interaction was detected equaled 1/2. Qualitatively one would have expected p to be less than the probability of detecting an interaction for two reasons:

1)   p refers to one delta ray only, whereas the interaction produces a number of charged secondaries.

2)   The delta rays that get out probably emerge from the matter close to the parent. There was matter less than 1/4" above some of the Geiger counters. Most delta rays made in this matter probably entered the same Geiger counter as did the parent.

Adjacent Geiger counter effect

Some alphas can pass obliquely through two adjacent Geiger counters. One can put an upper limit on the fraction which do this as follows: Consider the data obtained at sea level. If some alphas go through two adjacent Geiger counters, then the same percentage of mesons will also. In 5% of all sea level events more than one Geiger counter was tripped, and yet the pulse height corresponded to a single meson. About 2% of all mesons should have produced a delta ray in the matter beneath the lucite which tripped a second Geiger counter (see figure 24). Therefore, 3% seems to be an upper limit for the fraction of single particles which can pass obliquely through 2 adjacent Geiger counters.

In summary we have: $7 \pm 7\%$ of alphas produce interactions which trip 2 or more Geiger counters

                              $8 \pm 4\%$ of alphas produce delta rays which trip 2 or more Geiger counters

                              $\leq 3\%$ of alphas pass obliquely through 2 adjacent Geiger counters.

                              ————

                              $18 \pm 9\%$ of alphas will cause more than one Geiger counter to be triggered.

BIBLIOGRAPHY

1) P. Freier, E. J. Lofgren, E. P. Ney, F. Oppenheimer, H. L. Bradt,
   B. Peters   Phys. Rev. <u>74</u> 213 (1948)

2) E. Fermi   Phys. Rev. <u>75</u> 1169 (1949)

3) E. Fermi   The Astrophysical Journal <u>119</u> 1 (1954)

4) S. F. Singer   Phys. Rev. <u>80</u> 47 (1950)

5) L. Goldfarb, H. L. Bradt, B. Peters
   Phys. Rev. <u>77</u> 751 (1950)
   Progress of Cosmic Ray Physics, pg. 221
   (North Holland Publishing Company)

6) G. J. Perlow, L. R. Davis, C. W. Kissinger, J. D. Shipman, Jr.
   Phys. Rev. <u>88</u> 321 (1952)

7) S. F. Singer   Phys. Rev. <u>76</u> 701 (1949)

8) J. Linsley   Phys. Rev. <u>93</u> 899 (1954)
   (Corrected flux value was given to me in a
   private communication.)

9) E. P. Ney, D. M. Thon
   Phys. Rev. <u>81</u> 1069 (1951)

10) L. R. Davis, H. M. Caulk, C. Y. Johnson
    Phys. Rev. 91 431 (1953)
    (Corrected flux value was given to Dr. E. P. Ney
    in a private communication.)

11) F. B. McDonald   Private communication to Dr. E. P. Ney (1953)

12) M. F. Kaplon, B. Peters, H. L. Reynolds, D. M. Ritson
    Phys. Rev. <u>85</u> 295 (1952)

13) L. Bohl   To be published in Phys. Rev.

14) L. I. Schiff   Quantum Mechanics pg. 265
    (McGraw Hill Publishing Company)

15) J. R. Winckler, K. Anderson
    Phys. Rev. <u>93</u> 596 (1954)

16) B. R. Linden   Nucleonics <u>11</u> 31 (1953)

17) W. C. Elmore, M. Sands
    Electronics pg. 47 and 58
    (McGraw Hill Publishing Company)

18) A. M. Wood   Introduction to the Theory of Statistics pg. 61
    (McGraw Hill Publishing Company)

BIBLIOGRAPHY (Continued)

19) J. Linsley   Bull. Am. Phys. Soc. $\underline{29}$ 18 (1954)
                      Private communication

20) J. R. Winckler   Minutes of the Duke Conference (1953)

21) D. D. Montgomery Phys. Rev. $\underline{75}$ 1407 (1949)

22) F. L. Hereford   Phys. Rev. $\underline{77}$ 751 (1950)

Armed Services Technical Information Agency

Because of our limited supply, you are requested to return this copy WHEN IT HAS SERVED YOUR PURPOSE so that it may be made available to other requesters. Your cooperation will be appreciated.

AD
43707

UNCLASSIFIED